

# Equations of State for Mixtures of R-32, R-125, R-134a, R-143a, and R-152a

Eric W. Lemmon<sup>a)</sup>

Physical and Chemical Properties Division, National Institute of Standards and Technology, 325 Broadway,  
Boulder, Colorado 80305-3328

Richard T Jacobsen

Idaho National Engineering and Environmental Laboratory, P.O. Box 1625, Idaho Falls, Idaho 83415-2214

(Received 30 December 2002; revised manuscript received 16 December 2003; accepted 31 December 2003; published online 2 June 2004)

Mixture models explicit in Helmholtz energy have been developed to calculate the thermodynamic properties of refrigerant mixtures containing R-32, R-125, R-134a, R-143a, and R-152a. The Helmholtz energy of the mixture is the sum of the ideal gas contribution, the compressibility (or real fluid) contribution, and the contribution from mixing. The independent variables are the density, temperature, and composition. The model may be used to calculate the thermodynamic properties of mixtures, including dew and bubble point properties, within the experimental uncertainties of the available measured properties. It incorporates the most accurate equations of state available for each pure fluid. The estimated uncertainties of calculated properties are 0.1% in density and 0.5% in heat capacities and in the speed of sound. Calculated bubble point pressures have typical uncertainties of 0.5%. © 2004 by the U.S. Secretary of Commerce on behalf of the United States. All rights reserved. [DOI: 10.1063/1.1649997]

Key words: density; equation of state; heat capacity; HFC-32; HFC-125; HFC-134a; HFC-143a; HFC-152a; R-404A; R-407C; R-410A; R-507; refrigerant mixtures; speed of sound; thermodynamic properties; VLE.

## Contents

1. Introduction. . . . .	595
2. The Mixture Equation. . . . .	595
2.1. Vapor–Liquid Equilibrium (VLE) Properties. . . . .	597
3. Comparisons to Data. . . . .	598
3.1. The R-32/125 System. . . . .	602
3.2. The R-32/134a System. . . . .	604
3.3. The R-125/134a, R-125/143a, R-134a/143a, and R-134a/152a Systems. . . . .	606
3.4. The Ternary Mixtures. . . . .	607
3.5. Other Thermodynamic Properties. . . . .	610
4. Accuracy Assessment. . . . .	613
5. Acknowledgments. . . . .	619
6. References. . . . .	619

## List of Tables

1. Pure fluid equations of state for the refrigerants used in the mixture model. . . . .	596
2. Coefficients and exponents of the mixture equations. . . . .	596
3. Parameters of the mixture equations. . . . .	596
4. Coefficients and exponents of the ideal gas	

equations for the pure fluids. . . . .	598
5. Summary comparisons of mixture properties calculated from the model to refrigerant mixture data. . . . .	599
6. Calculated property values for computer code verification. . . . .	617

## List of Figures

1. Comparisons of densities calculated with the mixture model to experimental data for the R-32/125 binary mixture. . . . .	603
2. Comparisons of bubble point pressures calculated with the mixture model to experimental data for the R-32/125 binary mixture. . . . .	604
3. Comparisons of densities calculated with the mixture model to experimental data for the R-32/134a binary mixture. . . . .	605
4. Comparisons of bubble point pressures calculated with the mixture model to experimental data for the R-32/134a binary mixture. . . . .	606
5. Comparisons of densities calculated with the mixture model to experimental data for the R-125/134a binary mixture. . . . .	607
6. Comparisons of densities calculated with the mixture model to experimental data for the R-125/143a binary mixture. . . . .	608
7. Comparisons of densities calculated with the mixture model to experimental data for the	

<sup>a)</sup>Electronic mail: eric1@boulder.nist.gov

© 2004 by the U.S. Secretary of Commerce on behalf of the United States.  
All rights reserved.

R-134a/143a binary mixture. . . . .	609
8. Comparisons of densities calculated with the mixture model to experimental data for the R-134a/152a binary mixture. . . . .	610
9. Comparisons of bubble point pressures calculated with the mixture model to experimental data for the R-125/134a, R-125/143a, R-134a/143a, and R-134a/152a binary mixtures. . . . .	611
10. Comparisons of densities calculated with the mixture model to experimental data for the R-32/125/134a ternary mixture. . . . .	612
11. Comparisons of bubble point pressures calculated with the mixture model to experimental data for the R-32/125/134a and R-125/134a/143a ternary mixtures. . . . .	613
12. Comparisons of densities calculated with the mixture model to experimental data for the R-125/134a/143a ternary mixture. . . . .	614
13. Comparisons of isochoric heat capacities calculated with the mixture model to experimental data for the R-32/125, R-32/134a, R-125/134a, and R-125/143a binary mixtures. . . . .	615
14. Comparisons of isochoric heat capacities calculated with the mixture model to experimental data for the R-32/125/134a ternary mixture. . . . .	615
15. Comparisons of the speed of sound in the vapor phase calculated with the mixture model to experimental data for the R-32/125, R-32/134a, R-125/134a, and R-125/143a binary mixtures. . . . .	616
16. Comparisons of the speed of sound in the vapor phase calculated with the mixture model to experimental data for the R-32/125/134a ternary mixture. . . . .	616
17. Comparisons of the speed of sound in the liquid phase calculated with the mixture model to experimental data for the R-134a/152a binary mixture. . . . .	616
18. Isobaric heat capacity versus temperature diagram for an equimolar mixture of R-32 and R-125. . . . .	617
19. Comparisons of densities calculated with the mixture model developed in this work and the mixture model of Tillner-Roth <i>et al.</i> (1998) to experimental data for the R-32/125 binary mixture at 330 K. . . . .	618
20. Excess volumes for the R-32/125 binary mixture at 250 K and 5 MPa: (solid line) this work, (dashed line) mixture model of Tillner-Roth <i>et al.</i> (1998). Experimental data between 243 and 256 K are shown for comparison. . . . .	618
21. Excess enthalpies for the R-32/125 binary mixture at 250 K and 5 MPa: (solid line) this work, (dashed line) mixture model of Tillner-Roth <i>et al.</i> (1998). . . . .	618

## List of Symbols

<u>Symbol</u>	<u>Physical quantity</u>	<u>Unit</u>
$a$	Molar Helmholtz energy	J/mol
$A$	Helmholtz energy	J
$c_p$	Isobaric heat capacity	J/(mol·K)
$c_v$	Isochoric heat capacity	J/(mol·K)
$d$	Density exponent	
$f$	Fugacity	MPa
$F$	Generalized factor	
$g$	Gibbs energy	J/mol
$h$	Enthalpy	J/mol
$l$	Density exponent	
$m$	Number of components	
$M$	Molar mass	g/mol
$n$	Number of moles	mol
$p$	Pressure	MPa
$R$	Molar gas constant	J/(mol·K)
$s$	Entropy	J/(mol·K)
$t$	Temperature exponent	
$T$	Temperature	K
$u$	Internal energy	J/mol
$v$	Molar volume	dm <sup>3</sup> /mol
$V$	Volume	dm <sup>3</sup>
$w$	Speed of sound	m/s
$x$	Composition	mole fraction
$Z$	Compressibility factor ( $Z = p/\rho RT$ )	
$\alpha$	Reduced Helmholtz energy ( $\alpha = a/RT$ )	
$\delta$	Reduced density ( $\delta = \rho/\rho_c$ )	
$\rho$	Molar density	mol/dm <sup>3</sup>
$\tau$	Inverse reduced temperature ( $\tau = T_c/T$ )	
$\mu$	Chemical potential	J/mol
$\xi$	Reduced density parameter	dm <sup>3</sup> /mol
$\zeta$	Reduced temperature parameter	K
<b>Superscripts</b>		
0	Ideal gas property	
$E$	Excess property	
idmix	Ideal mixture	
$r$	Residual	
'	Saturated liquid state	
"	Saturated vapor state	
<b>Subscripts</b>		
0	Reference state property	
$c$	Critical point property	
calc	Calculated using an equation	
data	Experimental value	
$i,j$	Property of component $i$ or $j$	
red	Reducing parameter	

## 1. Introduction

The need for equations of state capable of accurate representation of thermodynamic properties of environmentally safe fluids continues as new applications are developed requiring the use of refrigerant mixtures. These mixtures of refrigerants are used as environmentally acceptable replacements for chlorofluorocarbons and hydrochlorofluorocarbons in refrigeration, heat pumps, foam-blowing, and other applications. Mixture equations are required to evaluate the performance of possible working fluids.

A model is presented here for calculating the thermodynamic properties of refrigerant mixtures that supercedes the model reported by Lemmon and Jacobsen (1999). This model was initially reported by Lemmon (1996), and general details and comparisons among different implementations of the model were reported by Lemmon and Tillner-Roth (1999). The model may be used to calculate all thermodynamic properties of mixtures at various compositions, including dew and bubble point properties and critical points; the model and its calculational abilities have been incorporated into the NIST REFPROP database (Lemmon *et al.*, 2002). The mixture model is similar to the model presented by Tillner-Roth *et al.* (1998) and published by the Japan Society of Refrigerating and Air Conditioning Engineers (JSRAE). The work presented here uses generalized equations applicable to several mixtures, whereas separate equations for each binary mixture were developed in the JSRAE equations.

The mixture model presented here is based on corresponding states theory and uses reducing parameters that are dependent on the mole fractions of the mixture constituents and critical points of the pure fluids to modify absolute values of the mixture density and temperature. This approach allows the thermodynamic properties of the mixture to be based largely on the contributions from the pure fluids. Without additional mixing functions, the model is similar to that for an ideal mixture, and only the excess values, or the departures from ideality, are required to accurately model the properties of the mixture.

The model uses the Helmholtz energy as the basis for all calculations. The Helmholtz energy is one of the fundamental properties from which all other thermodynamic properties can be calculated using simple derivatives. The Helmholtz energy of the mixture is calculated as the sum of an ideal gas contribution, a real fluid contribution, and a contribution from mixing. The Helmholtz energy from the contributions of the ideal gas and the real fluid behavior is determined at the reduced density and temperature of the mixture by the use of accurate pure fluid equations of state for the mixture components. Reducing parameters, dependent on the mole fractions of the constituents, are used to modify values of density and temperature for the mixture.

The contribution from mixing, a modified excess function, is given by an empirical equation. An excess property of a mixture is defined as the actual mixture property at a given condition minus the value for an ideal solution at the same

condition. In most other work dealing with excess properties, the mixing condition is defined at constant pressure and temperature. Because the independent variables for the pure fluid Helmholtz energy equations are reduced density and temperature, properties are calculated here at the reduced density and temperature of the mixture. The shape of the modified excess function is similar for many binary mixtures, and relatively simple scaling factors can be used to determine its magnitude for a particular application. While this approach is arbitrary and different from the usual excess property format, it results in an accurate representation of the single phase properties and phase boundaries.

The mixtures studied in this work include the constituents R-32 (difluoromethane), R-125 (pentafluoroethane), R-134a (1,1,1,2-tetrafluoroethane), R-143a (1,1,1-trifluoroethane), and R-152a (1,1-difluoroethane). Three separate models (i.e., three separate excess functions) were developed to calculate the properties of the refrigerant mixtures. The first two describe the properties of the binary mixtures R-32/125 and R-32/134a. The shapes of the excess functions for these two mixtures differ from each other and from those of the other mixtures studied in this work, and could not be modeled by a generalized equation. This was also noticed in the work of Lemmon (1996), which required additional terms in the mixing functions for these two binary mixtures. Laesecke (2004) noted that the electrical conductances of blends containing R-32 were much higher than other HFC blends. The higher conductance may be due to the polar R-32 molecules associating in the liquid phase via H-F bonds as suggested by Lisal and Vacek (1996).

The shapes of the excess functions for the mixtures R-125/134a, R-125/143a, R-134a/143a, and R-134a/152a were similar enough that one function could be developed that described the properties of all these systems. Additionally, experimental data for the ternary mixtures R-32/125/134a and R-125/134a/143a showed that only binary pair interactions are required to model these multicomponent mixtures.

## 2. The Mixture Equation

The equation for the mixture Helmholtz energy ( $a$ ) used in this work is

$$a = a^{\text{idmix}} + a^E. \quad (1)$$

The Helmholtz energy for an ideal mixture as used in this work defined in terms of density and temperature is

$$a^{\text{idmix}} = \sum_{i=1}^m x_i [a_i^0(\rho, T) + a_i^r(\delta, \tau) + RT \ln x_i], \quad (2)$$

where  $\rho$  and  $T$  are the mixture density and temperature,  $\delta$  and  $\tau$  are the reduced mixture density and temperature,  $m$  is the number of components in the mixture,  $a_i^0$  is the ideal gas Helmholtz energy of component  $i$ ,  $a_i^r$  is the residual Helmholtz energy of component  $i$ , and the  $x_i$  are the mole fractions of the mixture constituents. References for the pure fluid ideal gas Helmholtz energy and residual Helmholtz energy equations are given in Table 1.

TABLE 1. Pure fluid equations of state for the refrigerants used in the mixture model

Fluid	Author	Temperature range (K)	Maximum pressure (MPa)
R-32	Tillner-Roth and Yokozeki (1997)	136.34–435	70
R-125	Lemmon and Jacobsen (2004)	172.52–500	60
R-134a	Tillner-Roth and Baehr (1994)	169.85–455	70
R-143a	Lemmon and Jacobsen (2000)	161.34–650	100
R-152a	Outcalt and McLinden (1996)	154.56–500	60

The reduced values of density and temperature for the mixture models used here are

$$\delta = \rho / \rho_{\text{red}} \quad (3)$$

and

$$\tau = T_{\text{red}} / T, \quad (4)$$

where  $\rho$  and  $T$  are the mixture density and temperature, and  $\rho_{\text{red}}$  and  $T_{\text{red}}$  are the reducing values

$$\rho_{\text{red}} = \left[ \sum_{i=1}^m \frac{x_i}{\rho_{c_i}} + \sum_{i=1}^{m-1} \sum_{j=i+1}^m x_i x_j \xi_{ij} \right]^{-1} \quad (5)$$

and

$$T_{\text{red}} = \sum_{i=1}^m x_i T_{c_i} + \sum_{i=1}^{m-1} \sum_{j=i+1}^m x_i x_j \zeta_{ij}. \quad (6)$$

The parameters  $\zeta_{ij}$  and  $\xi_{ij}$  are used to define the shapes of the reducing temperature and density curves. These reducing parameters are not the same as the critical parameters of the mixture and are determined simultaneously in the nonlinear fit of experimental data with the other parameters of the mixture model. Additional values of  $\zeta_{ij}$  as well as a generalized method for predicting these values for refrigerants not covered in this work was given in Lemmon and McLinden (2001).

TABLE 2. Coefficients and exponents of the mixture equations

$k$	$N_k$	$t_k$	$d_k$	$l_k$
R-32/125				
1	-0.007 2955	4.5	2	1
2	0.078 035	0.57	5	1
3	0.610 07	1.9	1	2
4	0.642 46	1.2	3	2
5	0.014 965	0.5	9	2
6	-0.340 49	2.6	2	3
7	0.085 658	11.4	3	3
8	-0.064 429	4.5	6	3
R-32/134a				
1	0.229 09	1.9	1	1
2	0.094 074	0.25	3	1
3	0.000 398 76	0.07	8	1
4	0.021 113	2.0	1	2
R-125/134a, R-125/143a, R-134a/143a, R-134a/152a				
1	-0.013 073	7.4	1	1
2	0.018 259	0.35	3	1
3	0.000 008 1299	10.0	11	2
4	0.007 8496	5.3	2	3

Three excess functions were developed for the mixtures studied in this work. The excess function for the mixture Helmholtz energy for these three models is expressed as

$$\frac{a^E}{RT} = \alpha^E(\delta, \tau, \mathbf{x}) = \sum_{i=1}^{m-1} \sum_{j=i+1}^m x_i x_j F_{ij} \sum_k N_k \delta^{d_k} \tau^{t_k} \exp(-\delta^{l_k}). \quad (7)$$

Values of the coefficients and exponents of this equation are given in Table 2. The generalized factors and mixture parameters,  $F_{ij}$ ,  $\zeta_{ij}$  and  $\xi_{ij}$ , are given in Table 3.

The coefficients and exponents of Eq. (7) were obtained from nonlinear regression of experimental mixture data using fitting techniques similar to those applied to the development of the R-125 and R-143a equations of state given in Table 1. Additional details of the nonlinear fitting process are given in the respective papers for these two pure fluids. By including the exponents of Eq. (7) as nonlinear fitting parameters, the final equation was given additional degrees of freedom that are not normally available in linear least squares fits. In particular, the noninteger exponent  $t_k$  is flexible enough to decrease the number of terms required to achieve the same accuracy as fits from linear least squares applications. The physical behavior of the equation was carefully monitored during the fitting process using graphical techniques. Desirable characteristics of the final equation include the ability to produce correct calculated properties within the ranges of temperature and pressure defined by experimental data and to extrapolate to reasonable limits outside those experimental ranges. In addition, the equation is designed to exclude data which contain systematic behavior caused by experimental error.

For the most part, the mixture model was fitted to experimental values of single phase  $p$ - $\rho$ - $T$  and isochoric heat capacity data and a few selected values of the bubble point pressures. Since the calculation of the bubble point pressure

TABLE 3. Parameters of the mixture equations

Binary mixture	$\zeta_{ij}$ (K)	$\xi_{ij}$ ( $\text{dm}^3 \cdot \text{mol}^{-1}$ )	$F_{ij}$
R-32/125	28.95	-0.006 008	1.0
R-32/134a	7.909	-0.002 039	1.0
R-125/134a	-0.4326	-0.000 3453	1.0
R-125/143a	5.551	-0.000 4452	1.1697
R-134a/143a	2.324	0.000 6182	0.5557
R-134a/152a	4.202	0.004 223	2.0

requires an iterative solution, the number of fitted values was kept at a minimum, although comparisons were made to all values upon completion of each fit. The fitted data were carefully weighted such that a balance was obtained among the uncertainty of each data type (e.g., density versus heat capacity), the number of data points in a set, and the region where the data are located on the thermodynamic surface.

The equations used for calculating pressure ( $p$ ), compressibility factor ( $Z$ ), internal energy ( $u$ ), enthalpy ( $h$ ), entropy ( $s$ ), Gibbs energy ( $g$ ), isochoric heat capacity ( $c_v$ ), isobaric heat capacity ( $c_p$ ), and the speed of sound ( $w$ ) are given in Eqs. (8)–(15).

$$Z = \frac{p}{\rho RT} = 1 + \delta \left( \frac{\partial \alpha^r}{\partial \delta} \right)_\tau, \quad (8)$$

$$\frac{u}{RT} = \tau \left[ \left( \frac{\partial \alpha^0}{\partial \tau} \right)_\delta + \left( \frac{\partial \alpha^r}{\partial \tau} \right)_\delta \right], \quad (9)$$

$$\frac{h}{RT} = \tau \left[ \left( \frac{\partial \alpha^0}{\partial \tau} \right)_\delta + \left( \frac{\partial \alpha^r}{\partial \tau} \right)_\delta \right] + \delta \left( \frac{\partial \alpha^r}{\partial \delta} \right)_\tau + 1, \quad (10)$$

$$\frac{s}{R} = \tau \left[ \left( \frac{\partial \alpha^0}{\partial \tau} \right)_\delta + \left( \frac{\partial \alpha^r}{\partial \tau} \right)_\delta \right] - \alpha^0 - \alpha^r, \quad (11)$$

$$\frac{g}{RT} = 1 + \alpha^0 + \alpha^r + \delta \left( \frac{\partial \alpha^r}{\partial \delta} \right)_\tau, \quad (12)$$

$$\frac{c_v}{R} = -\tau^2 \left[ \left( \frac{\partial^2 \alpha^0}{\partial \tau^2} \right)_\delta + \left( \frac{\partial^2 \alpha^r}{\partial \tau^2} \right)_\delta \right], \quad (13)$$

$$\frac{c_p}{R} = \frac{c_v}{R} + \frac{\left[ 1 + \delta \left( \frac{\partial \alpha^r}{\partial \delta} \right)_\tau - \delta \tau \left( \frac{\partial^2 \alpha^r}{\partial \delta \partial \tau} \right)_\tau \right]^2}{\left[ 1 + 2\delta \left( \frac{\partial \alpha^r}{\partial \delta} \right)_\tau + \delta^2 \left( \frac{\partial^2 \alpha^r}{\partial \delta^2} \right)_\tau \right]}, \quad (14)$$

$$\frac{w^2 M}{RT} = \frac{c_p}{c_v} \left[ 1 + 2\delta \left( \frac{\partial \alpha^r}{\partial \delta} \right)_\tau + \delta^2 \left( \frac{\partial^2 \alpha^r}{\partial \delta^2} \right)_\tau \right], \quad (15)$$

The first derivative of pressure with respect to density at constant temperature ( $\partial p / \partial \rho$ )<sub>T</sub>, second derivative of pressure with respect to density at constant temperature ( $\partial^2 p / \partial \rho^2$ )<sub>T</sub>, and first derivative of pressure with respect to temperature at constant density ( $\partial p / \partial T$ )<sub>ρ</sub> are given in

$$\left( \frac{\partial p}{\partial \rho} \right)_T = RT \left[ 1 + 2\delta \left( \frac{\partial \alpha^r}{\partial \delta} \right)_\tau + \delta^2 \left( \frac{\partial^2 \alpha^r}{\partial \delta^2} \right)_\tau \right], \quad (16)$$

$$\left( \frac{\partial^2 p}{\partial \rho^2} \right)_T = \frac{RT}{\rho} \left[ 2\delta \left( \frac{\partial \alpha^r}{\partial \delta} \right)_\tau + 4\delta^2 \left( \frac{\partial^2 \alpha^r}{\partial \delta^2} \right)_\tau + \delta^3 \left( \frac{\partial^3 \alpha^r}{\partial \delta^3} \right)_\tau \right], \quad (17)$$

$$\left( \frac{\partial p}{\partial T} \right)_\rho = R\rho \left[ 1 + \delta \left( \frac{\partial \alpha^r}{\partial \delta} \right)_\tau - \delta \tau \left( \frac{\partial^2 \alpha^r}{\partial \delta \partial \tau} \right)_\tau \right]. \quad (18)$$

The ideal gas and residual Helmholtz energy required to calculate all single phase thermodynamic properties given in Eqs. (8)–(18) above are

$$\alpha^0 = \sum_{i=1}^m x_i \left[ \frac{a_i^0(\rho, T)}{RT} + \ln x_i \right] \quad (19)$$

and

$$\alpha^r = \sum_{i=1}^m x_i \alpha_i^r(\delta, \tau) + \alpha^E(\delta, \tau, \mathbf{x}), \quad (20)$$

where  $\alpha_i^r$  is the reduced residual Helmholtz energy of component  $i$ .

If equations for the ideal gas Helmholtz energy in the non-dimensional form  $a_i^0(\delta, \tau)$  are used rather than equations in the dimensional form  $a_i^0(\rho, T)$  as indicated by Eq. (19), the following reducing variables:

$$\delta = \rho / \rho_{c_i} \quad (21)$$

and

$$\tau = T_{c_i} / T, \quad (22)$$

rather than the reducing values defined by Eqs. (3) and (4), should typically be used in the ideal gas equation. [This does not apply to the residual part of the Helmholtz energy; the residual and excess terms  $\alpha_i^r(\delta, \tau)$  and  $\alpha^E(\delta, \tau, \mathbf{x})$  in Eq. (20) must be evaluated at the reduced state point of the mixture defined by Eqs. (3) and (4).] This complication is avoided through the use of the classical dimensional equations for functions involving the ideal gas heat capacity, such as

$$\begin{aligned} \alpha^0 = & -RT + RT \ln \frac{\rho T}{\rho_0 T_0} + h_{0i}^0 - T s_{0i}^0 + \int_{T_0}^T c_{pi}^0 dT \\ & - T \int_{T_0}^T \frac{c_{pi}^0}{T} dT. \end{aligned} \quad (23)$$

The following dimensional form (with density expressed in moles per cubic decimeter and temperature in Kelvins) and the associated coefficients given in Table 4 can be used for this purpose:

$$\begin{aligned} \frac{\alpha_i^0}{RT} = & e_1 + \frac{e_2}{T} + \ln \rho + (1 - c_0) \ln T - \sum_k c_k \left[ \frac{1}{t_k + 1} \right] \left[ \frac{1}{t_k} \right] T^{t_k} \\ & + \sum_k a_k \ln \left[ 1 - \exp \left( -\frac{b_k}{T} \right) \right]. \end{aligned} \quad (24)$$

Equations of the form

$$\alpha^0 = \ln \delta + N_0 \ln \tau + \sum_{i=1}^n N_i \tau^i + \dots \quad (25)$$

are derived from dimensional equations, and the critical parameters of the pure fluids are built into the coefficients of the equations. Additional information on the mixing function and its derivatives, as well as formulas for other thermodynamic properties, can be found in Lemmon *et al.* (2000), which presents an equation for mixtures of nitrogen, argon, and oxygen.

## 2.1. Vapor–Liquid Equilibrium (VLE) Properties

In a two-phase nonreacting mixture, the thermodynamic constraints for vapor–liquid equilibrium (VLE) are

$$T' = T'' = T, \quad (26)$$

TABLE 4. Coefficients and exponents of the ideal gas equations for the pure fluids

R-32	
$c_0 = 4.004\ 486$	
$a_1 = 1.160\ 761$	$b_1 = 798$
$a_2 = 2.645\ 151$	$b_2 = 4185$
$a_3 = 5.794\ 987$	$b_3 = 1806$
$a_4 = 1.129\ 475$	$b_4 = 115\ 10$
$e_1 = 7.254\ 707\ 84$	$e_2 = 2231.55735$
R-125	
$c_1 = 3.063$	$t_1 = 0.1$
$a_2 = 2.303$	$b_2 = 314.0$
$a_3 = 5.086$	$b_3 = 756.0$
$a_4 = 7.300$	$b_4 = 1707.0$
$e_1 = 29.876\ 6745$	$e_2 = 3013.2267$
R-134a	
$c_0 = -0.629\ 789$	
$c_1 = 0.377\ 018\ 08$	$t_1 = 0.5$
$c_2 = 0.060\ 585\ 489$	$t_2 = 0.75$
$e_1 = -12.280\ 8002$	$e_2 = 3385.257\ 07$
R-143a	
$c_1 = 1.0578$	$t_1 = 0.33$
$a_2 = 4.4402$	$b_2 = 1791$
$a_3 = 3.7515$	$b_3 = 823$
$e_1 = -1.577\ 780\ 74$	$e_2 = 2527.263\ 78$
R-152a	
$c_0 = 3.354\ 952$	
$c_1 = 0.010\ 986\ 49$	$t_1 = 1$
$c_2 = 2.501\ 616 \times 10^{-5}$	$t_2 = 2$
$c_3 = -2.787\ 445 \times 10^{-8}$	$t_3 = 3$
$e_1 = 4.360\ 056$	$e_2 = 2654.673\ 62$

$$p' = p'' = p, \quad (27)$$

and

$$\mu_i' = \mu_i'', \quad i = 1, 2, \dots, m, \quad (28)$$

where the superscripts ' and ', respectively, refer to the liquid and vapor phases. Equation (28) is equivalent to equating the fugacities of the coexisting liquid and vapor phases for each component in the mixture

$$f_i' = f_i''. \quad (29)$$

The chemical potential of component  $i$  in a mixture is

$$\mu_i(\rho, T) = \left( \frac{\partial A}{\partial n_i} \right)_{T, V, n_{j \neq i}} = \mu_i^c(T) + RT \ln(f_i), \quad (30)$$

where  $\mu_i^c(T)$  is a function of temperature only and the notation  $n_{j \neq i}$  indicates that all mole numbers are held constant except  $n_i$ . The chemical potential in an ideal gas mixture is

$$\mu_i^0 = \left( \frac{\partial A^0}{\partial n_i} \right)_{T, V, n_{j \neq i}} = \mu_i^c(T) + RT \ln(f_i^0), \quad (31)$$

where  $f_i^0$  is the ideal gas partial pressure of constituent  $i$ ,  $x_i p^0 = x_i \rho RT$ . Subtracting Eq. (30) from Eq. (31) and solving for  $f_i$  results in

$$f_i = x_i \rho RT \exp \left( \frac{\partial(n \alpha^r)}{\partial n_i} \right)_{T, V, n_{j \neq i}}, \quad (32)$$

where  $\alpha^r$  was defined in Eq. (20). The partial derivative at constant temperature, constant total volume (not molar volume), and constant mole numbers of all constituents except  $i$  is generally evaluated numerically.

### 3. Comparisons to Data

The uncertainties of calculated values of various properties are determined by comparisons with measured values. Statistical analyses are used to determine the overall estimated accuracy of the model, and to define the ranges of estimated uncertainties for various properties calculated with the formulation. Summary comparisons of values calculated using the mixture equation to data for  $p$ - $\rho$ - $T$ , heat capacity, and sound speed, as well as second virial coefficients and VLE information for refrigerant mixtures are given in Table 5, along with the temperature range of the data and the composition range for the first component listed. Bubble or dew point densities are included as  $p$ - $\rho$ - $T$  data, with the bubble or dew point pressure calculated from the mixture model. No further distinction is made between single phase densities and saturated densities. Compositions for VLE data are bubble point compositions except for datasets where only the vapor phase compositions were reported.

In a few cases, individual data points were eliminated from the comparisons when the deviation for a particular point was much higher than those for other points by the same author in the same region. For density, individual data points were typically deleted when the deviation exceeded 10%. This eliminates the likelihood of including in the comparisons data points that are in error or are reported incorrectly, including obvious typographical errors in published manuscripts. However, when the deviations slowly increased point by point, showing potentially systematic increasing differences in a particular region, these data points were left in the comparisons.

The statistics used to evaluate the equation are based on the percent deviation for any property,  $X$ ,

$$\% \Delta X = 100 \left( \frac{X_{\text{data}} - X_{\text{calc}}}{X_{\text{data}}} \right). \quad (33)$$

Using this definition, the average absolute deviation (AAD) in Table 5 is defined as

$$\text{AAD} = \frac{1}{n} \sum_{i=1}^n |\% \Delta X_i|, \quad (34)$$

where  $n$  is the number of data points. The comparisons given in the sections below for the various binary and ternary mixtures compare the equation of state to the experimental data by the use of the average absolute deviation as given by Eq. (34). Discussions of maximum errors or of systematic offsets always use the absolute values of the deviations.

TABLE 5. Summary comparisons of mixture properties calculated from the model to refrigerant mixture data

Author	No. points	Temperature range (K)	Pressure range (MPa)	Density range (mol/dm <sup>3</sup> )	Composition range (mole fraction) <sup>a</sup>	AAD <sup>b</sup> (%)
<b>R-32/125—<math>p\rho T</math></b>						
Benmansour and Richon (1997)	12 909	253–333	0.14–19.1	0.066–17.9	0.696	0.227
Benmansour and Richon (1999a)	26 777	253–333	0.108–20	0.049–18.3	0.093–0.885	0.627
Higashi (1997) <sup>c</sup>	23	323–346	3.01–5.07	1.98–10.7	0.497–0.776	5.01
Holcomb <i>et al.</i> (1998)	45	279–341	0.896–4.61	0.719–19.3	0.237–0.956	0.908
Kishizawa <i>et al.</i> (1999) <sup>c</sup>	34	339–344	3.90–4.90	4.47–8.62	0.204–0.700	5.67
Kiyoura <i>et al.</i> (1996)	94	330–440	1.83–5.24	0.829–1.72	0.367–0.606	0.134
Kleemiss (1997)	415	243–413	0.019–17.1	0.007–16.2	0.503–0.508	0.052
Magee (2002)	235	200–400	4.07–35.3	8.58–19.6	0.698	0.047
Magee and Haynes (2000)	228	200–400	2.57–35.3	1.06–17.4	0.5	0.040
Oguchi <i>et al.</i> (1995)	6	355–430	6.31–16.9	8.34–8.37	0.874	0.129
Perkins (2002)	411	300–398	3.85–19.1	6.54–14.8	0.698	0.116
Piao <i>et al.</i> (1996)	543	263–393	0.54–15	0.286–17.4	0.366–0.902	0.277
Sato <i>et al.</i> (1996)	156	320–440	1.78–5.27	0.836–1.72	0.698–0.902	0.140
Weber (2000)	90	295–334	1.45–3.98	0.777–16.9	0.416–0.885	0.627
Weber and Defibaugh (1994)	17	338–373	0.304–4.23	0.106–1.91	0.546	0.186
Widiatmo <i>et al.</i> (1993)	24	280–310	0.884–2.31	10.2–18.2	0.204–0.902	0.091
Zhang <i>et al.</i> (1996)	124	300–380	0.094–4.6	0.03–2.02	0.5–0.698	0.074
<b>R-32/125—VLE</b>						
Benmansour and Richon (1997)	18	253–333	0.385–3.83		0.696	1.27
Benmansour and Richon (1999a)	33	253–333	0.358–3.9		0.093–0.885	0.511
Defibaugh and Morrison (1995)	10	249–338	0.348–4.3		0.763	0.339
Fujiwara <i>et al.</i> (1992)	8	273	0.691–0.818		0.055–0.895	2.03
Higashi (1997)	22	283–313	0.906–2.48		0.225–0.896	0.473
Holcomb <i>et al.</i> (1998)	30	280–340	0.83–4.58		0.339–0.948	0.252
Kato <i>et al.</i> (2002)	39	318–349	2.35–5.27		0.111–0.953	1.85
Kleemiss (1997)	23	224–333	0.108–3.68		0.483–0.517	0.030
Nagel and Bier (1995)	34	205–345	0.038–5.05		0.241–0.951	0.415
Oguchi <i>et al.</i> (1995)	11	250–350	0.361–5.65		0.874	0.288
Piao <i>et al.</i> (1996)	10	263–283	0.54–1.07		0.366–0.902	0.701
Takagi <i>et al.</i> (1999)	47	248–333	0.284–3.93		0.269–0.941	0.999
Weber (2000)	90	295–334	1.45–3.98		0.416–0.885	0.270
Widiatmo <i>et al.</i> (1993)	24	280–310	0.884–2.31		0.204–0.902	0.338
<b>R-32/125—Second Virial Coefficient</b>						
Kiyoura <i>et al.</i> (1996)	23	330–440			0.367–0.606	2.21
Sato <i>et al.</i> (1996)	39	320–440			0.698–0.902	1.95
Weber and Defibaugh (1994)	3	338–373			0.546	3.15
<b>R-32/125—Isochoric Heat Capacity</b>						
Magee (2000a)	111	208–345		11.4–17.1	0.5	0.448
Perkins (2002)	363	300–397	4.13–18.3		0.698	1.74
<b>R-32/125—Isobaric Heat Capacity</b>						
Gunther and Steimle (1996)	89	203–313			0.434–0.874	0.855
<b>R-32/125—Sound Speed</b>						
Hozumi <i>et al.</i> (1995)	178	303–343	0.039–0.554		0.201–0.777	0.044
<b>R-32/134a—<math>p\rho T</math></b>						
Benmansour and Richon (1999b)	19 714	253–333	0.095–18.8	0.042–19.7	0.131–0.889	0.354
Higashi (1995) <sup>c</sup>	27	341–365	3.32–5.47	2.54–12.88	0.457–0.821	5.90
Holcomb <i>et al.</i> (1998)	44	279–340	0.523–4.29	0.805–17.2	0.13–0.973	1.13
Kleemiss (1997)	390	243–413	0.019–17.1	0.008–17.3	0.497–0.555	0.049
Magee and Haynes (2000)	461	200–400	2.7–35.5	1.1–18.5	0.329–0.5	0.075
Oguchi <i>et al.</i> (1999)	61	310–473	0.286–16.7	0.115–12.9	0.392–0.887	0.356
Oguchi <i>et al.</i> (1995)	53	238–473	0.135–15.3	2.01–18.8	0.274–0.71	0.237
Piao <i>et al.</i> (1996)	643	261–393	0.241–15	0.121–16.3	0.329–0.887	0.376
Sato <i>et al.</i> (1994)	220	320–440	1.97–6.18	1–2.12	0.329–0.887	0.208
Weber and Defibaugh (1994)	17	338–373	0.33–4.3	0.121–2.18	0.508	0.905
Widiatmo <i>et al.</i> (1994b)	30	280–340	0.577–3.1	11–18.6	0.329–0.887	0.173
Widiatmo <i>et al.</i> (1997)	22	280–330	1–3.01	12–14.7	0.395	0.110
<b>R-32/134a—VLE</b>						
Benmansour and Richon (1999b)	40	253–333	0.181–3.6		0.131–0.889	1.62
Chung and Kim (1997)	34	263–323	0.2–3.14		0.208–0.76	0.572
Defibaugh and Morrison (1995)	25	253–358	0.263–4.47		0.496–0.55	0.515
Fujiwara <i>et al.</i> (1992)	6	273	0.384–0.758		0.204–0.922	3.14

TABLE 5. Summary comparisons of mixture properties calculated from the model to refrigerant mixture data—Continued

Author	No. points	Temperature range (K)	Pressure range (MPa)	Density range (mol/dm <sup>3</sup> )	Composition range (mole fraction) <sup>a</sup>	AAD <sup>b</sup> (%)
Higashi (1995)	12	283–313	0.567–1.91		0.121–0.673	2.11
Holcomb <i>et al.</i> (1998)	48	280–340	0.379–4.56		0.162–0.783	0.428
Kim and Park (1999)	25	258–283	0.201–0.96		0.202–0.799	0.500
Kleemiss (1997)	16	223–343	0.073–3.15		0.419–0.517	0.345
Nagel and Bier (1995)	50	203–369	0.015–5.42		0.212–0.772	0.447
Oguchi <i>et al.</i> (1999)	36	243–361	0.173–5.02		0.392–0.887	2.45
Oguchi <i>et al.</i> (1995)	34	238–301	0.135–1.29		0.274–0.71	1.05
Piao <i>et al.</i> (1996)	10	261–283	0.241–0.93		0.329–0.887	0.412
Shimawaki <i>et al.</i> (2002)	40	263–293	0.252–1.4		0.135–0.923	0.493
Takagi <i>et al.</i> (1999)	35	243–333	0.084–3.34		0.184–0.808	2.06
Widiatmo <i>et al.</i> (1994b)	30	280–340	0.577–3.1		0.329–0.887	1.70
<b>R-32/134a—Second Virial Coefficient</b>						
Sato <i>et al.</i> (1994)	57	320–440			0.329–0.887	2.91
Tack and Bier (1997)	10	333–398			0.482–0.5	3.48
Weber and Defibaugh (1994)	3	338–373			0.508	7.74
<b>R-32/134a—Isochoric Heat Capacity</b>						
Magee (2000a)	131	205–343		13.2–18.4	0.5	0.311
<b>R32/134a—Isobaric Heat Capacity</b>						
Gunther and Steimle (1996)	96	203–323			0.397–0.882	1.43
<b>R-32/134a—Sound Speed</b>						
Hozumi <i>et al.</i> (1995)	193	303–343	0.031–0.241		0.155–0.896	0.016
<b>R-125/134a—<math>p\rho T</math></b>						
Benmansour and Richon (1999d)	11 153	253–303	0.034–20.3	0.016–13.4	0.131–0.942	0.252
Higashi (1999b) <sup>c</sup>	30	334–365	2.70–3.99	1.85–8.78	0.267–0.665	5.64
Holcomb <i>et al.</i> (1998)	17	280–342	0.537–2.55	0.529–11.9	0.35–0.72	0.237
Kleemiss (1997)	407	243–413	0.019–17.1	0.008–13.2	0.5–0.51	0.046
Magee and Haynes (2000)	268	200–400	2.84–35.5	1.66–14.1	0.5	0.103
Weber and Defibaugh (1994)	18	303–373	0.17–4.03	0.069–2.22	0.495	0.266
Widiatmo <i>et al.</i> (1997)	149	280–350	1–3.02	8–12.4	0.087–0.923	0.086
Yokoyama <i>et al.</i> (2000)	341	298–423	0.101–6.62	0.029–4.49	0.251–0.751	0.817
<b>R-125/134a—VLE</b>						
Benmansour and Richon (1999d)	23	253–303	0.147–1.5		0.131–0.942	1.41
Higashi (1999b)	15	283–313	0.517–1.73		0.179–0.776	1.10
Higuchi and Higashi (1995)	25	283–313	0.412–2		0.179–0.776	0.848
Holcomb <i>et al.</i> (1998)	40	280–340	0.379–3.63		0.259–0.649	0.554
Kim and Park (1999)	35	263–303	0.201–1.57		0–0.814	0.552
Kleemiss (1997)	24	224–343	0.066–2.9		0.461–0.514	0.302
Nagel and Bier (1995)	31	206–365	0.017–3.97		0.254–0.749	0.278
Widiatmo <i>et al.</i> (1997)	36	280–350	0.425–2.97		0.087–0.923	1.28
<b>R-125/134a—Second Virial Coefficient</b>						
Weber and Defibaugh (1994)	4	323–373			0.495	2.53
<b>R-125/134a—Isochoric Heat Capacity</b>						
Magee (2000a)	94	206–345		10–14	0.5	0.375
<b>R-125/134a—Isobaric Heat Capacity</b>						
Gunther and Steimle (1996)	73	203–323			0.222–0.719	0.877
<b>R-125/134a—Sound Speed</b>						
Hozumi (1996)	81	303–343	0.041–0.529		0.349–0.694	0.020
<b>R-125/143a—<math>p\rho T</math></b>						
Higashi (1999c) <sup>c</sup>	30	325–342	2.44–3.71	1.99–8.98	0.412–0.620	2.25
Holcomb <i>et al.</i> (1998)	14	280–328	0.798–2.56	0.612–11.5	0.35–0.672	0.997
Ikeda and Higashi (1995) <sup>c</sup>	14	325–344	2.46–3.71	2.29–8.98	0.412	2.13
Kishizawa <i>et al.</i> (1999) <sup>c</sup>	19	340–344	3.45–3.71	2.94–6.89	0.412	3.95
Kleemiss (1997)	151	243–373	1.6–17.1	6.41–13.2	0.504	0.037
Magee and Haynes (2000)	281	200–400	2.13–35.4	0.881–14.1	0.5	0.075
Uchida <i>et al.</i> (1999) <sup>c</sup>	7	308–341	1.65–3.48	0.931–3.03	0.412	0.951
Weber and Defibaugh (1994)	27	333–373	0.218–3.27	0.08–1.45	0.509	0.329
Widiatmo <i>et al.</i> (1994a) <sup>c</sup>	37	280–330	0.1–0.199	8.16–11.8	0.073–0.863	0.245
Zhang <i>et al.</i> (1998)	205	305–390	0.115–4.76	0.037–2.53	0.273–0.737	0.136
<b>R-125/143a—VLE</b>						
Higashi (1999c)	18	273–313	0.622–2.01		0.151–0.759	1.60
Holcomb <i>et al.</i> (1998)	36	280–326	0.767–2.64		0.287–0.65	0.833
Kleemiss (1997)	16	223–338	0.086–3.3		0.461–0.499	0.306
Nagel and Bier (1996)	19	205–343	0.032–3.69		0.493–0.503	0.136

TABLE 5. Summary comparisons of mixture properties calculated from the model to refrigerant mixture data—Continued

Author	No. points	Temperature range (K)	Pressure range (MPa)	Density range (mol/dm <sup>3</sup> )	Composition range (mole fraction) <sup>a</sup>	AAD <sup>b</sup> (%)
Uchida <i>et al.</i> (1999)	7	308–341	1.65–3.47		0.412	0.301
Widiatmo <i>et al.</i> (1994a)	34	280–330	0.773–2.83		0.073–0.863	0.805
<b>R-125/143a—Second Virial Coefficient</b>						
Tack and Bier (1997)	6	333–398			0.493–0.515	7.42
Uchida <i>et al.</i> (1999)	8	330–400			0.412	4.66
Weber and Defibaugh (1994)	5	333–373			0.509	5.29
<b>R-125/143a—Isochoric Heat Capacity</b>						
Magee (2000a)	109	205–344		9.89–14	0.5	0.550
<b>R-125/143a—Isobaric Heat Capacity</b>						
Gunther and Steimle (1996)	73	203–318			0.193–0.671	0.832
<b>R-125/143a—Sound Speed</b>						
Ichikawa <i>et al.</i> (1998)	142	303–343	0.04–0.549		0.2–0.803	0.011
<b>R-134a/143a—<math>p\rho T</math></b>						
Holcomb <i>et al.</i> (1998)	17	280–343	0.522–2.82	0.662–12.3	0.282–0.65	1.34
Kleemiss (1997)	377	243–413	0.092–17.1	0.032–13.9	0.492–0.501	0.053
<b>R-134a/143a—VLE</b>						
Higuchi (1997)	9	273–313	0.388–1.6		0.294–0.751	3.80
Holcomb <i>et al.</i> (1998)	40	280–340	0.379–3.32		0.35–0.835	0.540
Kim <i>et al.</i> (2000)	54	263–313	0.2–1.83		0.079–0.92	0.418
Kleemiss (1997)	18	223–354	0.059–3.39		0.502–0.522	0.144
Kubota and Matsumoto (1993)	41	278–333	0.35–2.88		0.145–0.891	0.951
Lim <i>et al.</i> (2002)	35	273–313	0.294–1.83		0.081–0.905	0.756
Nagel and Bier (1996)	12	205–361	0.021–3.94		0.504–0.526	0.680
<b>R-134a/152a—<math>p\rho T</math></b>						
Dressner and Bier (1993)	139	333–423	0.281–56	0.083–12.1	0.485–0.538	0.196
Tillner-Roth (1993)	1721	243–433	0.089–16.9	0.028–15.3	0.248–0.751	0.053
Weber and Defibaugh (1994)	11	353–373	0.268–3.17	0.094–1.69	0.497	0.160
<b>R-134a/152a—VLE</b>						
Defibaugh and Morrison (1995)	13	248–368	0.104–3.43		0.777	0.719
Kleiber (1994)	25	255–298	0.131–0.662		0.315–0.978	0.826
Sand <i>et al.</i> (1994)	4	273	0.271–0.286		0.118–0.758	2.44
Tillner-Roth (1993)	23	313–378	0.926–4.09		0.23–0.75	0.258
<b>R-134a/152a—Second Virial Coefficient</b>						
Schramm <i>et al.</i> (1992)	7	233–473				11.2
Weber and Defibaugh (1994)	2	353–373			0.497	5.40
<b>R-134a/152a—Isobaric Heat Capacity</b>						
Gunther and Steimle (1996)	32	203–323			0.138–0.72	2.64
Tuerk <i>et al.</i> (1996)	49	298–423	0.1–2.5		0.5	0.370
<b>R-134a/152a—Sound Speed</b>						
Beliajeva <i>et al.</i> (1999)	329	230–350	0.456–16.5		0.128–0.688	0.265
Grebenkov <i>et al.</i> (1994)	120	230–336	0.57–19		0.688	0.267
<b>R-32/125/134a—<math>p\rho T</math></b>						
Benmansour and Richon (1998)	11 623	253–333	0.12–15.2	0.058–15.5	0.377	0.162
Benmansour and Richon (1999c)	4067	253–303	0.028–17.1	0.012–15	0.105–0.469	0.276
Higashi (1999a) <sup>c</sup>	16	341–359	3.27–4.64	2.64–10.4	0.381	7.47
Holcomb <i>et al.</i> (1998)	42	244–346	0.229–3.93	0.711–15.3	0.2–0.676	1.57
Hurly <i>et al.</i> (1997)	88	313–453	0.321–7.79	0.086–2.76	0.346	0.213
Ikedo and Higashi (1995)	16	341–359	3.27–4.10	2.64–10.4	0.381	6.81
Kiyoura <i>et al.</i> (1996)	105	315–440	1.57–5.75	0.767–2.07	0.381–0.515	0.587
Kleemiss (1997)	369	243–413	0.026–17.1	0.009–15.4	0.334–0.348	0.083
Magee (2000b)	352	200–400	2.97–35.2	1.58–17.1	0.334–0.381	0.119
Oguchi <i>et al.</i> (1995)	12	365–430	5.19–12.4	5.86–6.22	0.38–0.471	0.202
Piao <i>et al.</i> (1996)	1025	263–393	0.447–15	0.209–15.2	0.186–0.473	0.282
Widiatmo <i>et al.</i> (1997)	76	280–340	0.724–3.24	10.4–14.9	0.347–0.464	0.196
<b>R-32/125/134a—VLE</b>						
Benmansour and Richon (1998)	18	253–333	0.212–2.72		0.377	2.14
Benmansour and Richon (1999c)	9	253–303	0.25–1.39		0.105–0.335	2.21
Higuchi (1997)	72	273–323	0.556–2.73		0.173–0.54	0.927
Holcomb <i>et al.</i> (1998)	58	221–345	0.073–3.93		0.045–0.599	0.919
Kleemiss (1997)	44	222–353	0.074–4.2		0.144–0.661	0.356
Nagel and Bier (1995)	29	205–362	0.026–4.77		0.187–0.434	0.253
Piao <i>et al.</i> (1996)	31	270–326	0.448–2.41		0.317–0.381	0.650
Widiatmo <i>et al.</i> (1997)	20	280–340	0.724–3.24		0.347–0.464	0.951

TABLE 5. Summary comparisons of mixture properties calculated from the model to refrigerant mixture data—Continued

Author	No. points	Temperature range (K)	Pressure range (MPa)	Density range (mol/dm <sup>3</sup> )	Composition range (mole fraction) <sup>a</sup>	AAD <sup>b</sup> (%)
<b>R-32/125/134a—Second Virial Coefficient</b>						
Hozumi <i>et al.</i> (1995)	11	340–440			0.23	8.48
Kiyoura <i>et al.</i> (1996)	11	340–440			0.381	2.76
<b>R-32/125/134a—Isochoric Heat Capacity</b>						
Magee (2000b)	147	203–345		11.5–17.1	0.334–0.381	0.280
<b>R-32/125/134a—Isobaric Heat Capacity</b>						
Gunther and Steimle (1996)	48	203–318			0.346–0.381	0.766
<b>R-32/125/134a—Sound Speed</b>						
Hozumi (1996)	27	303–343	0.045–0.537		0.34	0.016
Hurly <i>et al.</i> (1997)	361	260–400	0.051–0.982		0.346	0.009
<b>R-125/134a/143a—<math>p\rho T</math></b>						
Bouchot and Richon (1998)	1644	253–333	0.004–18.7	0.002–13.1	0.358	0.292
Fujiwara <i>et al.</i> (1998)	162	263–403	1.5–15	0.482–12.8	0.358	0.301
Kleemiss (1997)	196	243–373	1.4–17.1	6.15–13.4	0.341	0.034
<b>R-125/134a/143a—VLE</b>						
Bouchot and Richon (1998)	16	253–333	0.3–2.88		0.358	0.486
Higuchi (1997)	22	273–313	0.597–1.88		0.338–0.356	1.23
Kleemiss (1997)	26	224–345	0.07–3.15		0.316–0.331	0.247
Nagel and Bier (1996)	13	205–364	0.017–3.96		0.159–0.172	0.578
<b>R-125/134a/143a—Isobaric Heat Capacity</b>						
Gunther and Steimle (1996)	24	203–318			0.358	1.69

<sup>a</sup>Composition range is listed for the first component.

<sup>b</sup>Average absolute deviation in density for  $p$ – $\rho$ – $T$  data and in bubble point pressure for VLE data. For second virial coefficients, numbers given are average absolute differences (cm<sup>3</sup>/mol).

<sup>c</sup>Saturated liquid or vapor densities.

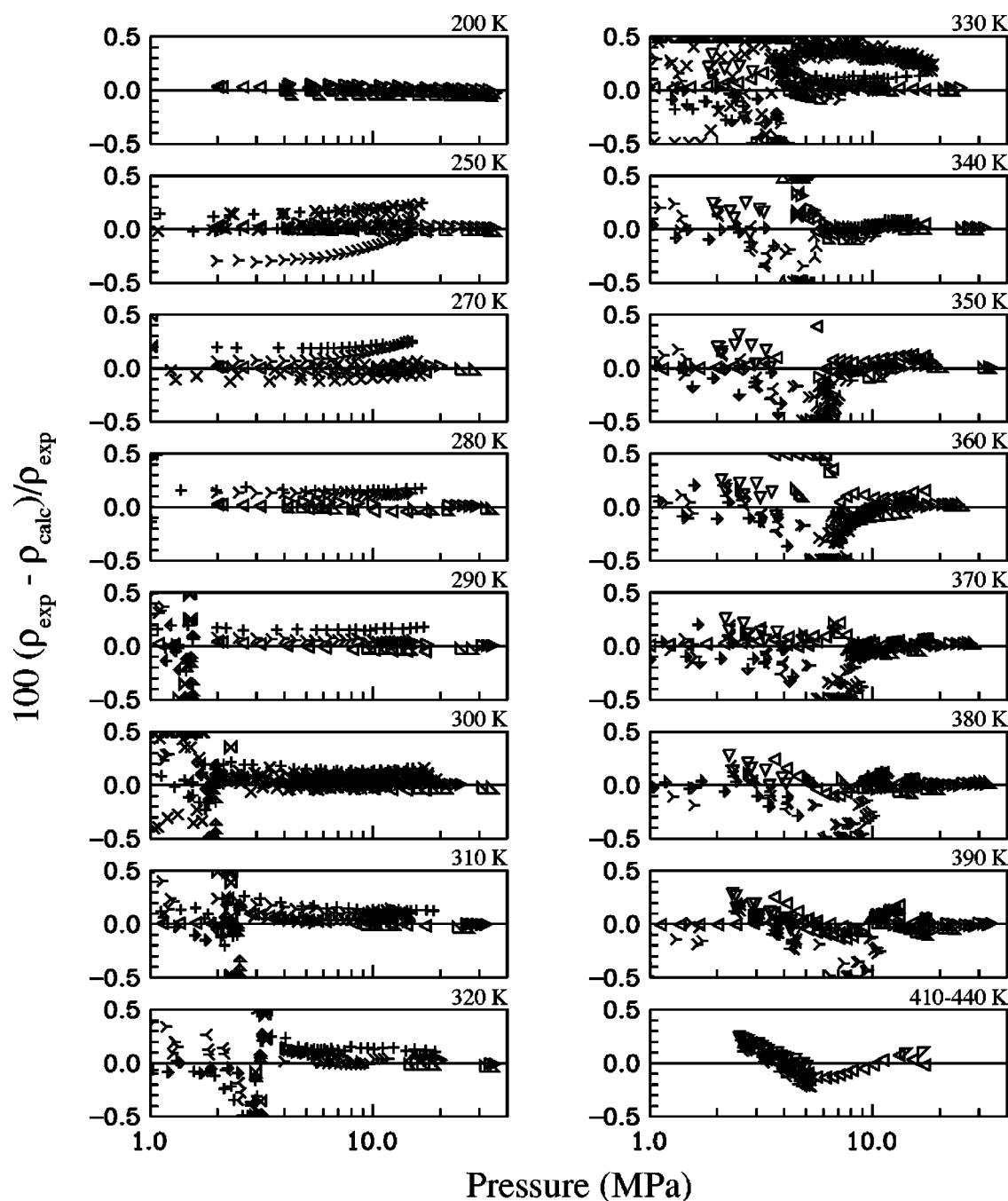
The comparisons of the mixture model to experimental data exhibit many general trends, as shown in the figures presented in this section. In these figures, data of a given type are separated into temperature increments of 10 K, where the temperatures listed at the top of each small plot are the lower bounds of these ranges. Comparisons to  $p\rho T$  data focus for the most part on deviations in density, given inputs of pressure and temperature. However, in the critical region, deviations in density are generally higher than in the liquid or vapor phase at states away from the critical point, and several of the systems described below include comparisons based on deviations in pressure, given inputs of density and temperature. Such comparisons are typical for equations of state for both pure fluids and mixtures, and are not specific to the model presented here. The artificially large deviations are an artifact in the calculation of deviations caused by the fact that  $dp/d\rho$  is nearly zero in the critical region. For the VLE data, the comparisons given in the following sections focus on the relative deviation in bubble point pressure. There are some VLE systems for which only the vapor phase compositions were reported, and the relative deviation in bubble point pressure is replaced with the relative deviation in dew point pressure in such cases.

### 3.1. The R-32/125 System

The R-32/125 system is perhaps the most widely studied system of all mixtures that have ever been measured, even compared to the well measured systems methane/ethane, nitrogen/argon, and dry air. The data span the entire compo-

sition range and were measured at temperatures and pressures that cover nearly the entire range of practical fluid states. Further experimental data for the region at temperatures above 380 K would be of use for verifying the accuracy of the mixture model in this region.

Comparisons of experimental density data for the R-32/125 binary mixture to the mixture model are shown in Fig. 1. For the datasets of Benmansour and Richon (1997, 1999a), only one out of every 50 points is shown due to the very large number of data points published by these authors. All of the temperature, pressure, and composition ranges covered by Benmansour and Richon are shown in the figures, but the smaller set used for plotting allows the symbol shapes to be seen in the plots. In the liquid phase at temperatures below 360 K, the datasets of Kleemiss (1997), Magee and Haynes (2000), and Magee (2002) are represented on average to within 0.03%. The equation represents the data of Widiatmo *et al.* (1993), Piao *et al.* (1996), Perkins (2002), and Weber and Defibaugh (1994) with average deviations of 0.1%. Comparisons with the data of Benmansour and Richon (1997, 1999a) show slightly higher deviations (about 0.17%). The data of Benmansour and Richon (1999a) (in the liquid phase) agree favorably with the equation, except for the data at 330 K, which have a systematic offset of about 0.3% and do not agree with other data at this temperature. The AAD for this dataset in the liquid is 0.06% if the data at 330 K are omitted. The data of Piao *et al.* show systematic offsets near 263 and 273 K (disagreeing with other data in the same region and composition), but the average differences fall to 0.08% at higher temperatures.



+ Benmansour and Richon (1997)  
 \* Higashi (1997)  
 Δ Kishizawa *et al.* (1999)  
 ◁ Kleemiss (1997)  
 ▽ Magee and Haynes (2000)  
 ⋈ Perkins (2002)  
 < Sato *et al.* (1996)  
 ↓ Weber and Defibaugh (1994)  
 ↗ Zhang *et al.* (1996)

× Benmansour and Richon (1999a)  
 ⊠ Holcomb *et al.* (1998)  
 ▾ Kiyoura *et al.* (1996)  
 ▷ Magee (2002)  
 ▹ Oguchi *et al.* (1995)  
 > Piao *et al.* (1996)  
 † Weber (2000)  
 ‡ Widiatmo *et al.* (1993)

FIG. 1. Comparisons of densities calculated with the mixture model to experimental data for the R-32/125 binary mixture.

The scatter between various experimental datasets is much higher in the vapor region than in the liquid. Calculated values from the equation exhibit deviations between 0.02% and 0.18% on average from the data of Kleemiss (1997) (0.02%),

Kiyoura *et al.* (1996), Sato *et al.* (1996), Weber and Defibaugh (1994), and Zhang *et al.* (1996). Differences are greater for other datasets.

Above 360 K, deviations in the area near the critical point

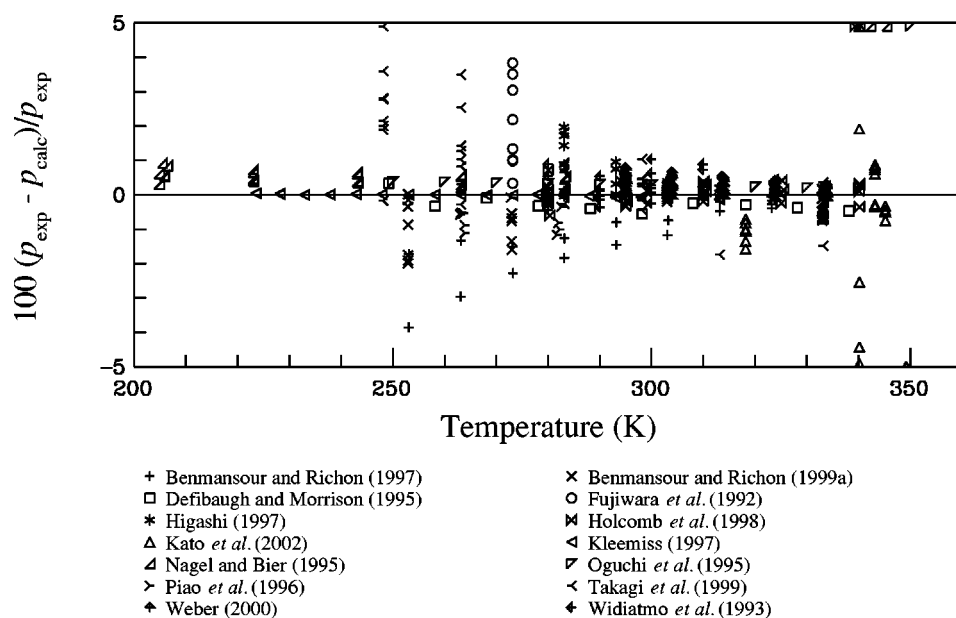


FIG. 2. Comparisons of bubble point pressures calculated with the mixture model to experimental data for the R-32/125 binary mixture.

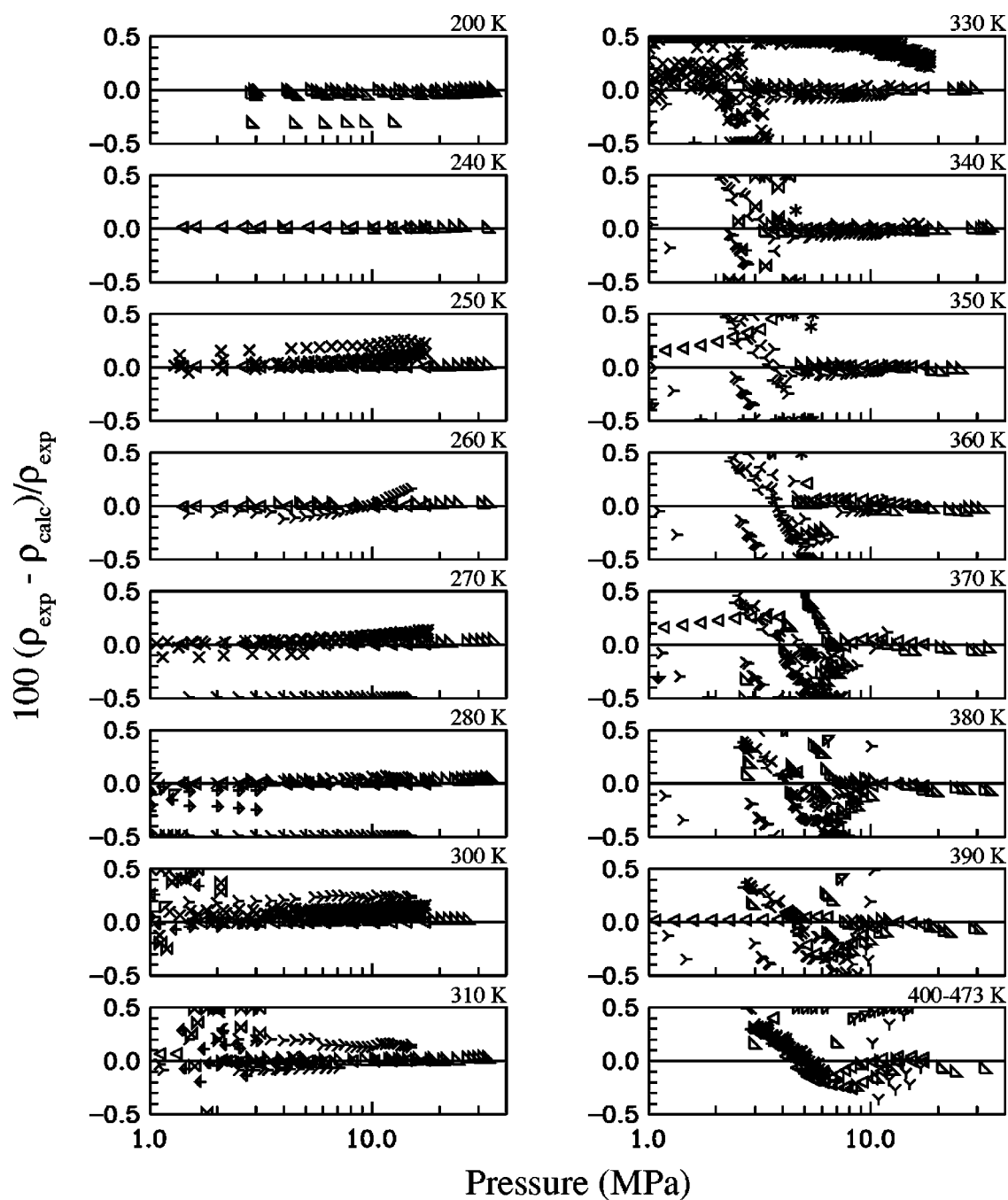
and at higher temperatures tend to increase, with the maximum errors in the datasets of Kiyoura *et al.* (1996) and Sato *et al.* (1996) reaching 0.3% in density. Comparisons with the data of Kleemiss (1997) show smaller differences, but even for this dataset, the model shows offsets of 0.15% at the highest temperatures. As stated previously, in the close vicinity of the critical point, it is not useful to compare deviations in density, because a slight error in pressure in this region can be accompanied by large errors in the density, with differences easily exceeding 5%. Deviations in pressure are more meaningful as a measure of the physical behavior of the model. Above 340 K, the average absolute deviation in pressure is approximately 0.1% for all datasets. Even as the critical points of the mixtures at different compositions are approached (339–351 K, 3.6–5.8 MPa), the maximum deviations do not exceed approximately 0.3% in pressure. For the commercial mixture R-410A (the 50/50 by mass mixture of R-32 and R-125), there are four datasets within the region 4–10 mol/dm<sup>3</sup>: Kishizawa *et al.* (1999), Magee (2002), Perkins (2002), and Piao *et al.* (1996), with the data of Kishizawa *et al.* and of Perkins measured near the critical point. The equation shows close agreement with the data of Perkins, with an average deviation of 0.16% in density (including the very near critical region) and 0.07% in pressure.

Comparisons to bubble point pressures are shown in Fig. 2. Eliminating the data points that fall substantially outside the main body of VLE data in terms of their deviations from the mixture model, bubble point pressures are represented on average to within 0.4%. The data of Kleemiss (1997), which are represented with an AAD of 0.05%, were the primary data used in the development of the model given here. However, nearly all of the other data points from various authors are represented within a band of  $\pm 1\%$ . Other datasets that agree well with the data of Kleemiss include those of Defibaugh and Morrison (1995), 0.26%; Holcomb *et al.* (1998), 0.27%; Weber (2000), 0.32%; Oguchi *et al.* (1995),

0.36%; and Widiatmo *et al.* (1993), 0.4%. No systematic offsets are seen in the comparisons. In the few cases where both bubble and dew point compositions are given, differences between the calculated and experimental dew point compositions are generally within 0.005 mole fraction, where the dew point compositions (and mixture pressure) were calculated given the mixture temperature and bubble point compositions.

### 3.2. The R-32/134a System

Comparisons of calculated mixture densities to experimental density data for the R-32/134a binary mixture are shown in Fig. 3. For the dataset of Benmansour and Richon (1999b), only one out of every 20 points is shown (similar to that for the R-32/125 mixture) due to the very large number of data points published by these authors. The data of Kleemiss (1997) and of Magee and Haynes (2000) are represented on average to within 0.06%. Between 210 and 360 K, the average representation is 0.024%. The data of Magee and Haynes between 200 and 210 K for the 0.33 mole fraction of R-32 show an offset of 0.3%; similar offsets were seen in other models, including that of Tillner-Roth *et al.* (1998) published by the JSRAE, and in the earlier model of Lemmon and Jacobsen (1999). The liquid phase data of Benmansour and Richon are represented with an average difference of 0.09% (excluding the data at 330 K, similar to that done for the R-32/125 mixture). The vapor phase data of Kleemiss at 370 and 390 K cannot both be represented simultaneously within the stated experimental accuracy of the data. In this work, the equation is biased towards the data at 390 K, causing the higher deviations of calculated values at 370 K. Excluding the data at 273 and 283 K (which appear to be in



× Benmansour and Richon (1999b)  
 ⊠ Holcomb *et al.* (1998)  
 ▴ Magee and Haynes (2000)  
 ∇ Oguchi *et al.* (1999)  
 ◀ Sato *et al.* (1994)  
 † Widiatmo *et al.* (1994b)

\* Higashi (1995)  
 ◁ Kleemiss (1997)  
 ▽ Oguchi *et al.* (1995)  
 ▷ Piao *et al.* (1996)  
 ‡ Weber and Defibaugh (1994)  
 † Widiatmo *et al.* (1997)

FIG. 3. Comparisons of densities calculated with the mixture model to experimental data for the R-32/134a binary mixture.

error with deviations greater than 1%) at a composition of 0.45 mole fraction of R-32, values from the equation deviate from the data of Piao *et al.* below 360 K on average by 0.21%. The data of Piao *et al.* above 360 K show increasing scatter due to the complexity of modeling and measuring the

critical region. Below 330 K in the vapor phase, the data of Oguchi *et al.* (1995) and Widiatmo *et al.* (1994b, 1997) show average deviations of 0.1%. Above 330 K, in the area around the critical region, the scatter in the data and the deviations from the equation increase substantially. Devia-

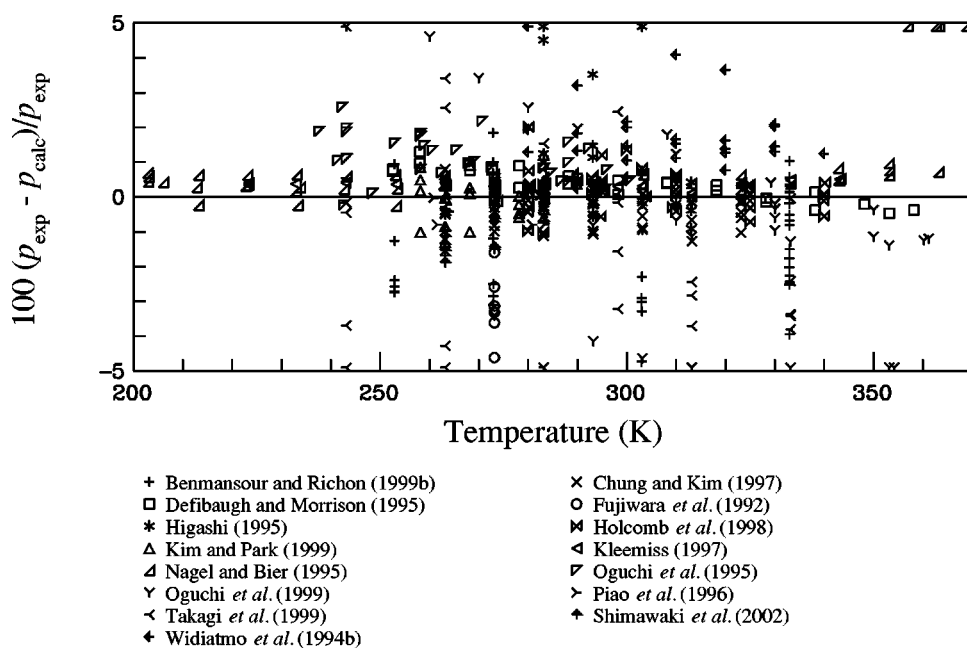


FIG. 4. Comparisons of bubble point pressures calculated with the mixture model to experimental data for the R-32/134a binary mixture.

tions between the equation and the data of Oguchi *et al.* (1995, 1999), Sato *et al.* (1994), and Weber and Defibaugh (1994) are about 0.3%, including some systematic differences.

Comparisons to VLE data (see Fig. 4) for the R-32/134a system show nearly the same trends as those for the R-32/125 system. In a similar fashion (eliminating the extraneous data points outside the main group of data), VLE data are generally represented with an AAD of 0.6%. All of the datasets appear to be of similar quality. Average differences are 0.38%, 0.41%, 0.50%, and 0.57% for the datasets of Takagi *et al.* (1999), Piao *et al.* (1996), Kim and Park (1999), and Chung and Kim (1997), respectively. For those datasets that reported both liquid and vapor composition, differences for each data point in the dew point composition are generally about 0.006 mole fraction.

### 3.3. The R-125/134a, R-125/143a, R-134a/143a, and R-134a/152a Systems

Calculated densities are compared to the experimental data for the R-125/134a binary mixture in Fig. 5. As was done with the R-32/134a mixture, only one out of every 20 points are shown for the dataset of Benmansour and Richon (1999d). The data of Kleemiss (1997) and of Magee and Haynes (2000) are represented on average to within 0.07%. Below 360 K, the average deviation is 0.05%. In the liquid phase at 240 K, there is a systematic offset of 0.06% compared to the data of Kleemiss. This offset decreases quickly with increasing temperature. The model deviates from the data of Benmansour and Richon in the liquid by 0.11%. In the vapor phase, the average absolute deviation of the equation from the data of Widiatmo *et al.* (1997) is 0.09%. At the highest temperatures above the critical point, differences from the data of Kleemiss increase to a maximum of 0.26%

at pressures around the critical pressure. Similar trends are found in the JSRAE model by Tillner-Roth *et al.* (1998) at the high temperatures, but with a maximum deviation of 0.20%.

Comparisons of calculated values to the experimental density data for the R-125/143a binary mixture are shown in Fig. 6. Differences between the equation and the data of Kleemiss (1997) and of Magee and Haynes (2000) are around 0.06%. Below 360 K, differences fall (on average) to 0.03% for these two datasets. In the vapor phase, comparisons with the data of Widiatmo *et al.* (1994a), Weber and Defibaugh (1994), and Zhang *et al.* (1998) show differences of 0.17%.

Comparisons for the R-134a/143a system are shown in Fig. 7. Below 360 K, comparisons with the equation show differences (on average) of 0.03% in both the liquid and vapor phases from the data of Kleemiss (1997). Above 360 K, the differences increase at pressures near the critical pressure of the mixture, but decrease to an average deviation of 0.1% in density at lower and higher pressures, including the data in the critical region. Similar comments can be made about the R-134a/152a system (see Fig. 8). Differences below 360 K, as well as at conditions above 360 K away from the critical pressure of the mixture, are about 0.06%. As the critical region is approached, differences increase up to 0.5%. Although there are few publications of measurements for this system, it was covered in detail by Tillner-Roth (1993) for a wide range of temperature and pressure, and for several compositions (0.25, 0.50, and 0.75 mole fraction). These data are well represented by the model reported here.

The comparisons to VLE data for the R-125/134a, R-125/143a, and R-134a/143a binary mixtures (see Fig. 9) are similar to those described above for the R-32/125 and R-32/134a systems. The average absolute deviation for each system is approximately 0.5% in bubble point pressure. Comparisons with the dew point compositions are similar to those for the

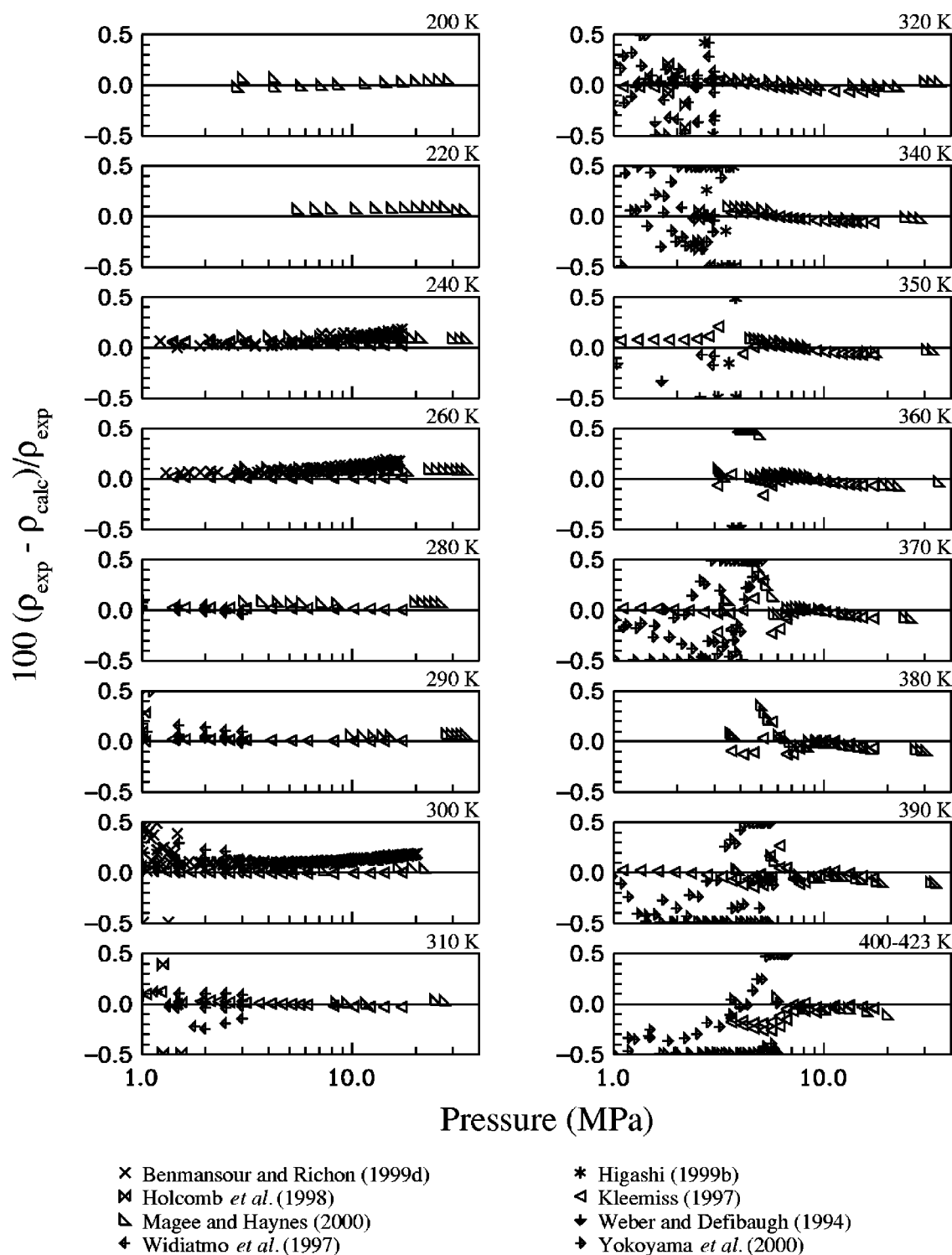


FIG. 5. Comparisons of densities calculated with the mixture model to experimental data for the R-125/134a binary mixture.

other systems previously described. The R-134a/152a system shows similar trends above 270 K, but at lower temperatures there is a systematic offset of calculated bubble point pressures compared to the data of Defibaugh and Morrison (1995) and of Kleiber (1994), with a maximum difference of 2.4% in pressure for both of these datasets.

### 3.4. The Ternary Mixtures

The R-32/125/134a system is unique from a modeling standpoint since it combines the three mixture equations (the individual equations for R-32/125 and R-32/134a, and the generalized equation for R-125/134a). No additional param-

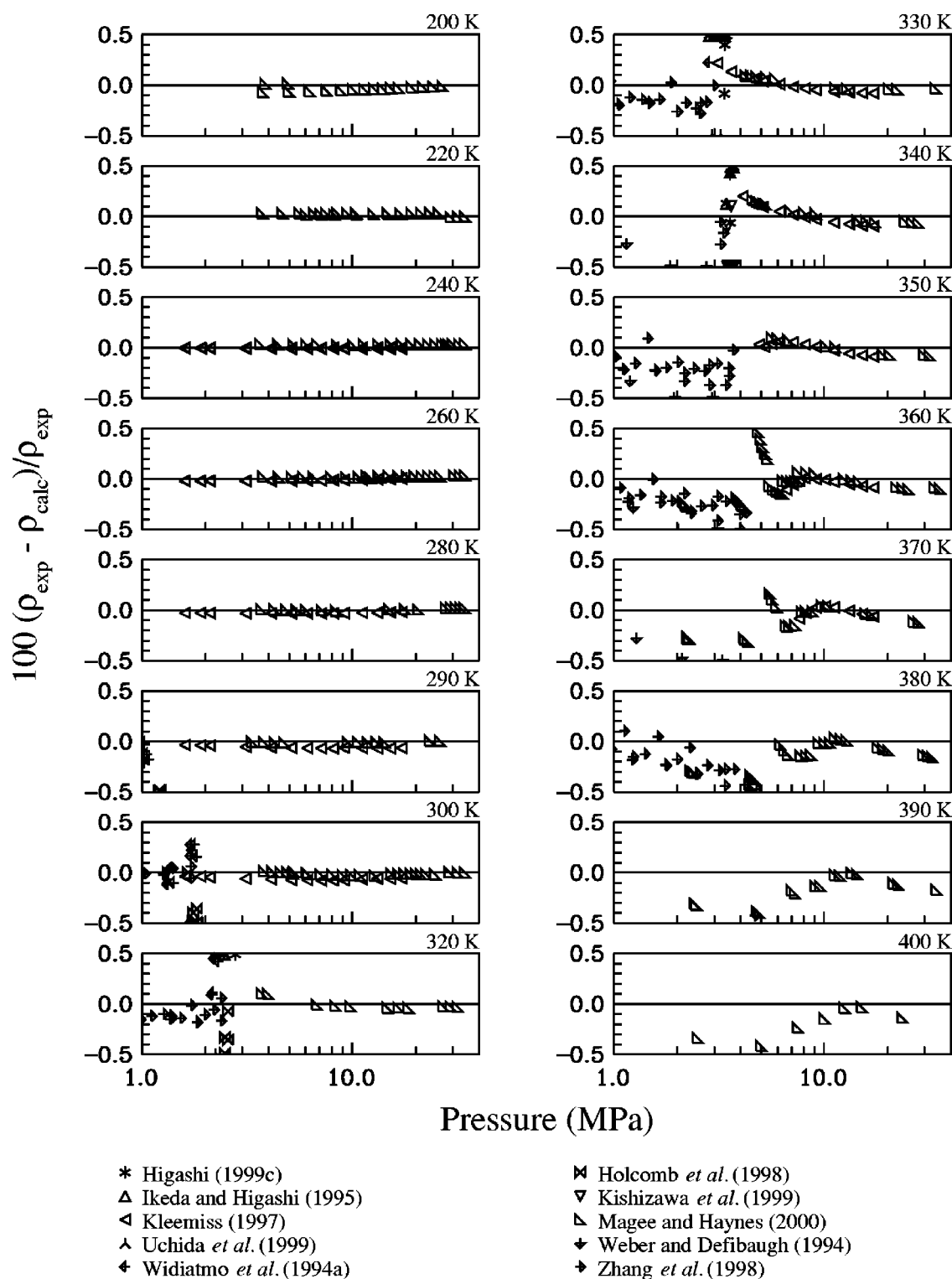


FIG. 6. Comparisons of densities calculated with the mixture model to experimental data for the R-125/143a binary mixture.

eters were required to model the ternary mixture, although slight systematic offsets are seen in several locations. Comparisons of the combined mixture model for this ternary mixture are shown in Fig. 10. Similar to the R-32/125 mixture, only one out of every 20 points is shown for the datasets of Benmansour and Richon (1998, 1999c). In the liquid region

below 360 K, the equations represent the data of Magee (2000b) and Kleemiss (1997) with an average deviation of 0.05%. At temperatures near 260 K, systematic offsets of 0.04% and 0.08% are seen for the datasets of Kleemiss and Magee, respectively. The liquid data of Benmansour and Richon (1998) are represented by average deviations of

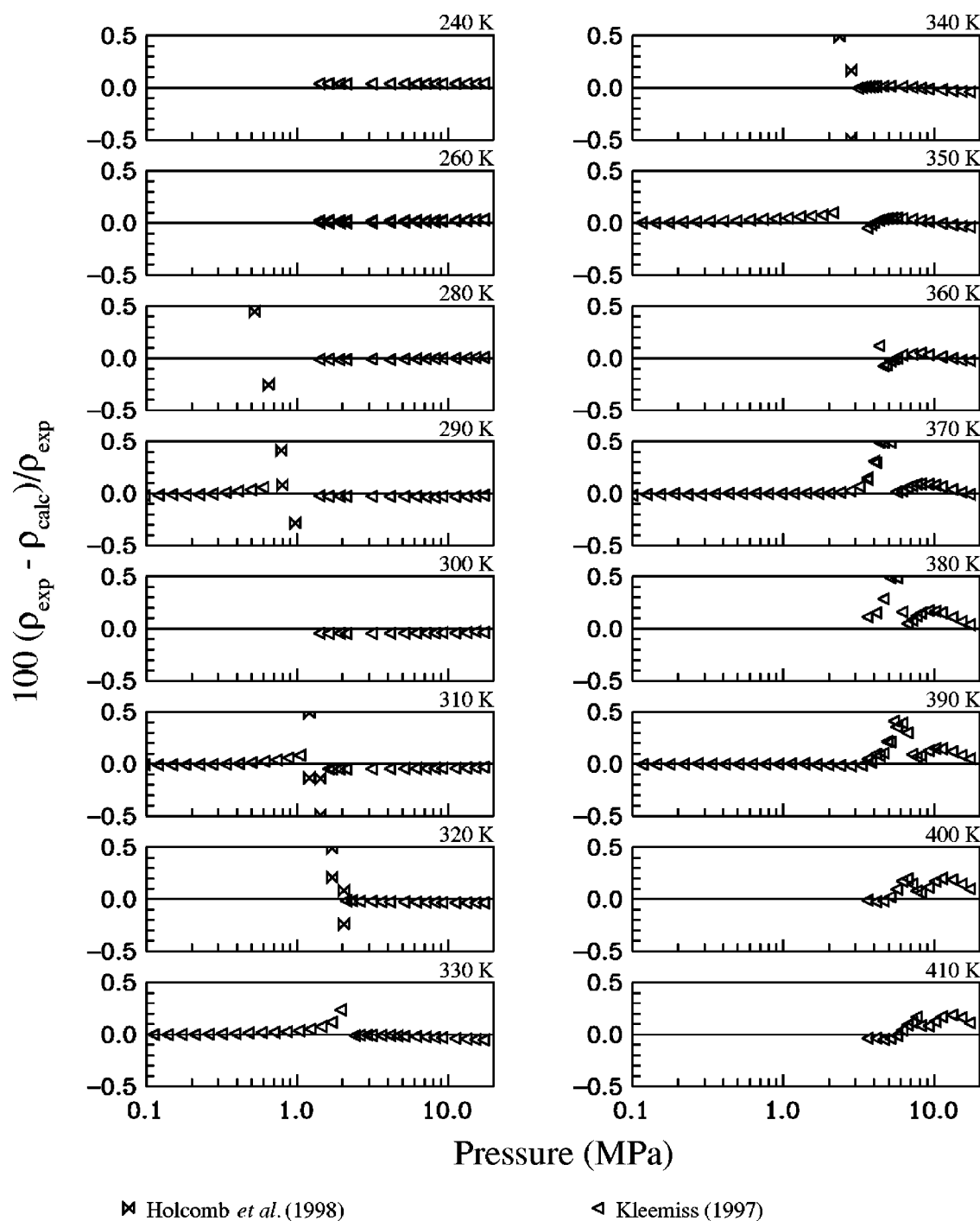


FIG. 7. Comparisons of densities calculated with the mixture model to experimental data for the R-134a/143a binary mixture.

0.05% when the data at 330 K are eliminated (as was done with the R-32/125 mixture). In the vapor region (below 360 K), differences are about 0.06% for the data of Kleemiss, but increase to 0.5% for the data of Benmansour and Richon (1998) and of Piao *et al.* (1996). Above 360 K, differences continue to increase, with maximum deviations of 0.5% for the data of Kleemiss and higher for other datasets. The scatter among data sets of various authors is greater than 0.5% in density near the critical region as expected.

Figure 11 illustrates comparisons of VLE data for the

R-32/125/134a ternary mixture. Bubble point pressures are represented on average to within 0.7% and dew point composition differences are within 0.005 mole fraction of R-32. Comparisons to the data of Nagel and Bier (1995) show deviations of 0.26% and those with Piao *et al.* (1996) show deviations of 0.66%.

Although the ternary mixture R-125/134a/143a has no additional fitted parameters, the properties of this system are represented with accuracies similar to those of the binary mixtures. The experimental data of Kleemiss (1997) are rep-

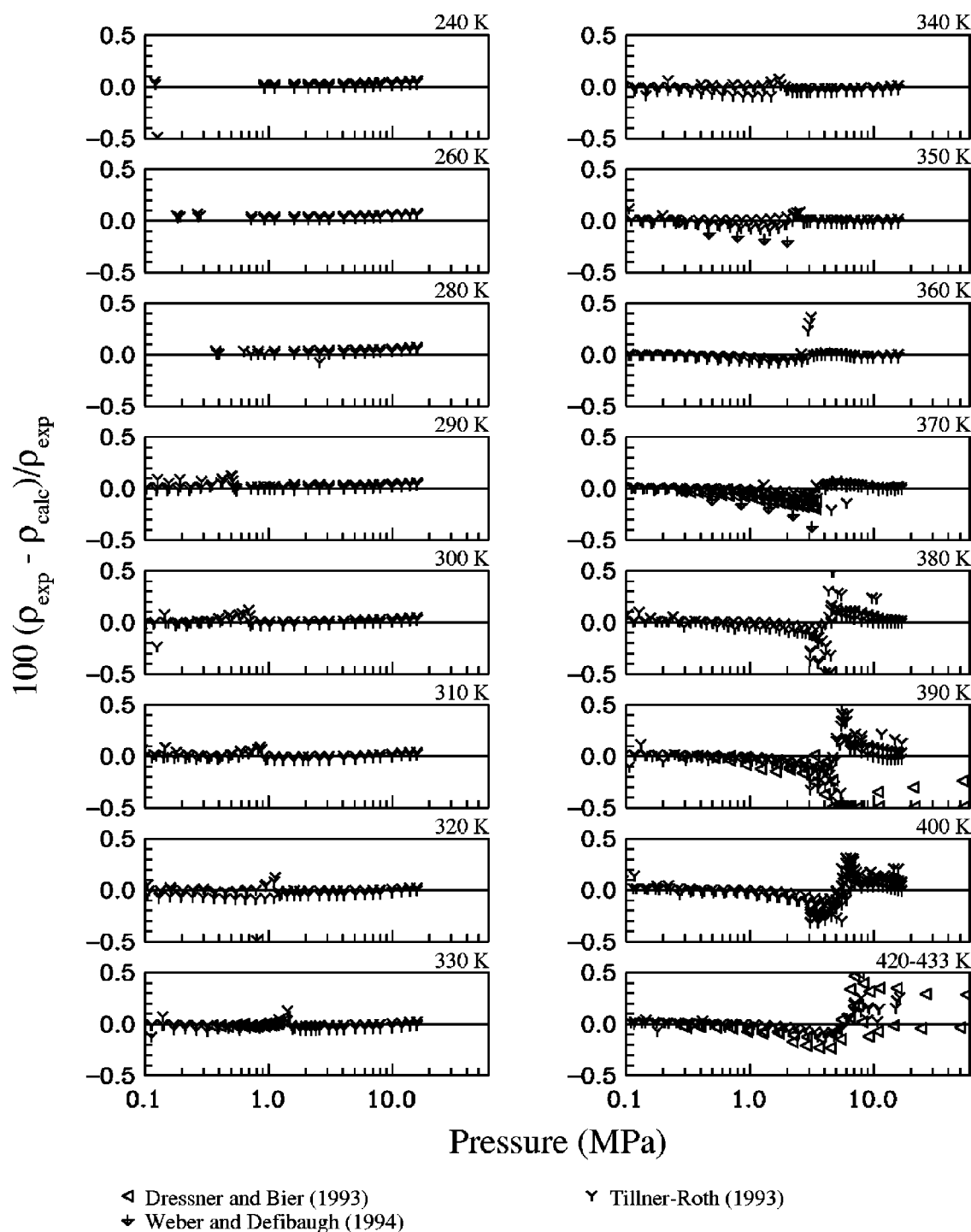


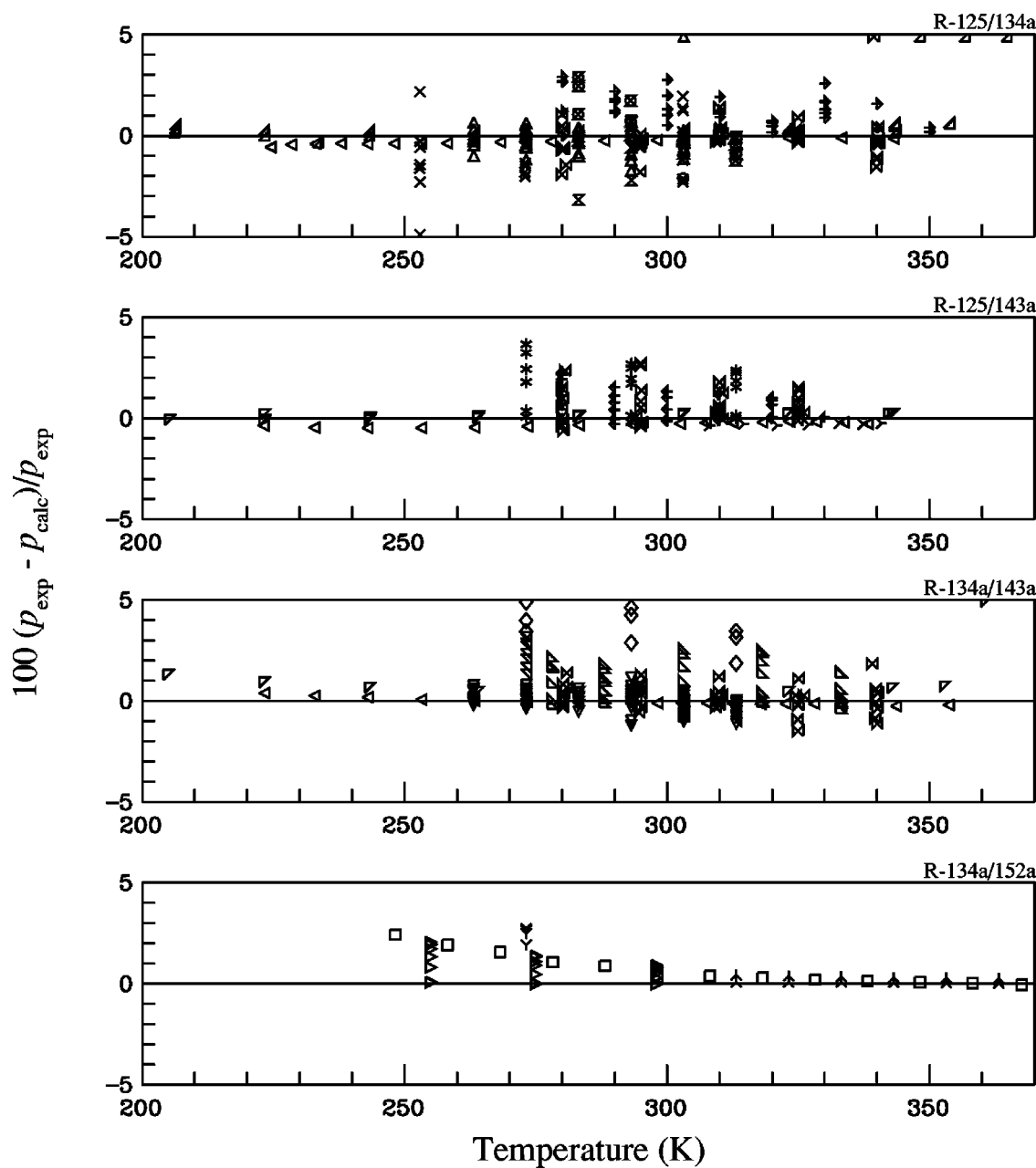
FIG. 8. Comparisons of densities calculated with the mixture model to experimental data for the R-134a/152a binary mixture.

resented on average by differences of 0.03%. Deviations for the data of Bouchot and Richon (1998) in the liquid phase are 0.09%. Small systematic differences are evident in the comparisons given in Fig. 12, such as the offset of 0.05% at 300 K. Trends above 360 K in the critical region are similar to those described for the binary mixtures above. Figure 11 also includes comparisons of VLE data for the R-125/134a/143a ternary mixture. There are very few phase equilibrium data for this mixture, but the data of Nagel and Bier (1996)

and those of Kleemiss (1997) are in agreement within about 1% in bubble point pressure, with an AAD of 0.35%.

### 3.5. Other Thermodynamic Properties

The isochoric heat capacity has been measured by Magee (2002) and Perkins (2002) for four of the binary mixtures: R-32/125, R-32/134a, R-125/134a, and R-125/143a. Figure 13 compares values calculated from the model to these data.



- |                                  |                                 |
|----------------------------------|---------------------------------|
| × Benmansour and Richon (1999d)  | □ Defibaugh and Morrison (1995) |
| ○ Higashi (1999b)                | * Higashi (1999c)               |
| ◇ Higuchi (1997)                 | ⊠ Higuchi and Higashi (1995)    |
| ⊠ Holcomb <i>et al.</i> (1998)   | △ Kim and Park (1999)           |
| ▽ Kim <i>et al.</i> (2000)       | ◁ Kleemiss (1997)               |
| ▷ Kleiber (1994)                 | ▴ Kubota and Matsumoto (1993)   |
| ▽ Lim <i>et al.</i> (2002)       | △ Nagel and Bier (1995)         |
| ▽ Nagel and Bier (1996)          | Y Sand <i>et al.</i> (1994)     |
| ^ Tillner-Roth (1993)            | > Uchida <i>et al.</i> (1999)   |
| ⋄ Widiatmo <i>et al.</i> (1994a) | ⋄ Widiatmo <i>et al.</i> (1997) |

FIG. 9. Comparisons of bubble point pressures calculated with the mixture model to experimental data for the R-125/134a, R-125/143a, R-134a/143a, and R-134a/152a binary mixtures.

In addition, comparisons to the experimental data for the R-32/125/134a ternary mixture are shown in Fig. 14. In general, the mixture model represents the data with an average absolute deviation between 0.3% and 0.5% for the binary

mixtures, and 0.3% for the ternary mixture. There is very little systematic behavior in the deviations for the systems studied, and the model represents the data to within their experimental uncertainty.

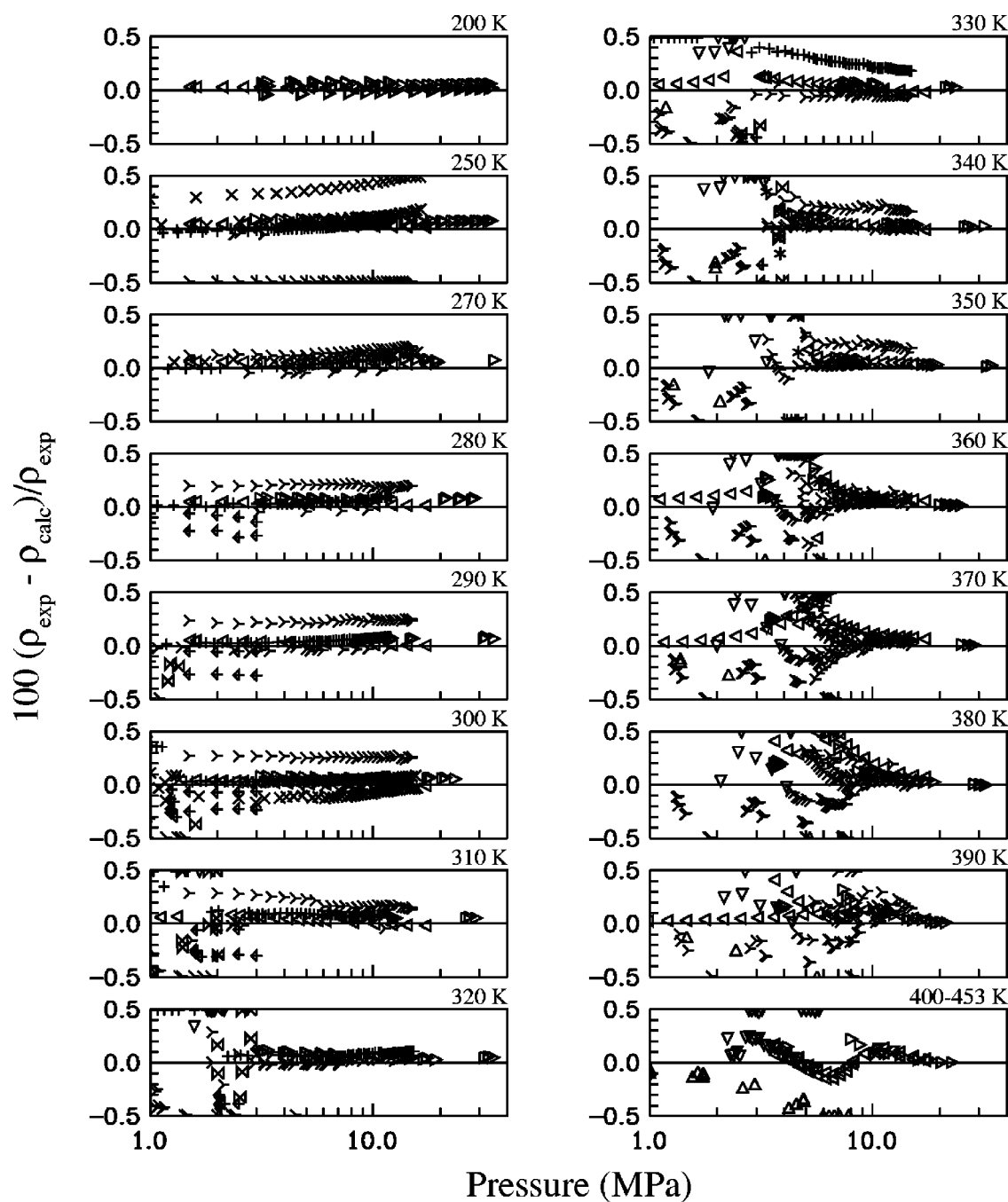


FIG. 10. Comparisons of densities calculated with the mixture model to experimental data for the R-32/125/134a ternary mixture.

Comparisons to the saturated liquid isobaric heat capacity data of Gunther and Steimle (1996) for the seven mixtures that they studied show comparable deviations, with differences generally less than 1% for most of the mixtures, except at the lowest temperatures (200 K) and near the critical re-

gion (where  $c_p$  tends to increase rapidly with increasing temperature). The R-134a/152a system is the only exception, with deviations of less than 1% at the highest temperatures, but with steadily increasing deviations at lower temperatures, with a maximum of 5% at 200 K. This is the only system

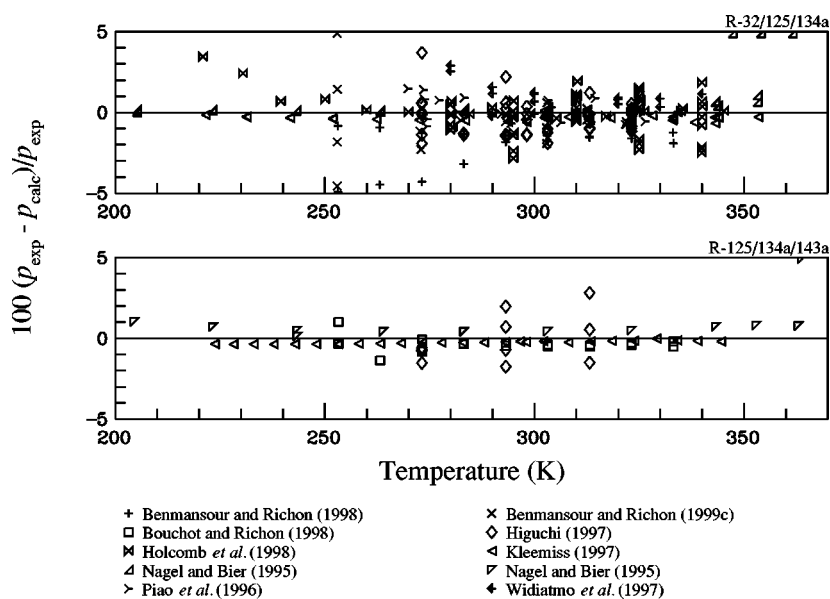


FIG. 11. Comparisons of bubble point pressures calculated with the mixture model to experimental data for the R-32/125/134a and R-125/134a/143a ternary mixtures.

with vapor measurements, and the model represents these data (Tuerk *et al.*, 1996) with an average absolute deviation of 0.37%.

Speed of sound measurements in the vapor phase for the R-32/125, R-32/134a, R-125/134a, R-125/143a, and R-32/125/134a mixtures were given by Hozumi (1996), Hurly *et al.* (1997), and Ichikawa *et al.* (1998). Comparisons of the model to these data are shown in Fig. 15 for the binary mixtures and Fig. 16 for the ternary mixture. The average absolute deviations for these systems range between 0.01% and 0.04% in the speed of sound. In the liquid phase of the R-134a/152a system, the mixture model represents the speed of sound measurements of Beliajeva *et al.* (1999) and Grebenkov *et al.* (1994) within an average absolute deviation of about 0.3%, as shown in Fig. 17.

#### 4. Accuracy Assessment

Based on comparisons to experimental data, the uncertainties of the equation are generally 0.1% in density, 0.5% in heat capacity and speed of sound, and 0.5% for calculated bubble point pressures. The model is valid from 200 to 450 K up to 60 MPa as verified by experimental data. Although the equation was developed using mostly binary data, it is accurate in calculating the properties of the two ternary mixtures for which data were available for comparison. It is expected that this result will apply to other ternary and higher-order systems as well. Table 6 gives calculated values from the model for computer code verification.

Graphical analyses of various properties were made to verify the behavior of the equations over their ranges of validity, especially for heat capacities in the liquid region, and to test the extrapolation behavior of the equations. Figure 18 shows a typical example of the isobaric heat capacity as applied to the equimolar mixture of R-32 and R-125 (or

R-410A). Plots for the isochoric heat capacity and speed of sound showed similar physically correct behavior for different systems at various compositions.

Future measurements are needed to confirm whether the equation is valid for predicting properties of other mixtures and for calculating properties of states in regions not covered by the experimental data used in the development of this model. Such data will enable continued evaluation and refinement of the model and modeling process. While early measurements of mixture properties were considered to be less accurate than those for pure substances, modern mixture data are now approaching the accuracy of measurements for the pure fluids. Refinements in the equations of state for both pure substances and mixtures will improve the prediction of properties for fluid mixtures as they become more common as working fluids in engineered systems.

Comparisons were made to determine the sensitivity of the mixture model to the accuracies of the pure fluid equations of state used in its formulation. Two highly accurate equations are available for R-143a: the equation of Lemmon and Jacobsen (2000) used in this work and the equation of Li *et al.* (1999). The deviations between the equations and the experimental data are similar for both equations, and the behavior of derived properties such as the heat capacities show similar trends. Replacing the equation of Lemmon and Jacobsen with the equation of Li *et al.* showed virtually no change in the deviations for the R134a/143a binary mixture in terms of density or bubble point pressure. Likewise, differences between the two equations for calculated values of heat capacity and speed of sound are less than 0.2% for the binary mixture.

There are also two highly accurate equations available for R-125, the equation of Lemmon and Jacobsen (2004) and the equation of Sunaga *et al.* (1998). The equation of Lemmon and Jacobsen uses a new form of the equation of state to eliminate the large calculated pressures (both negative and

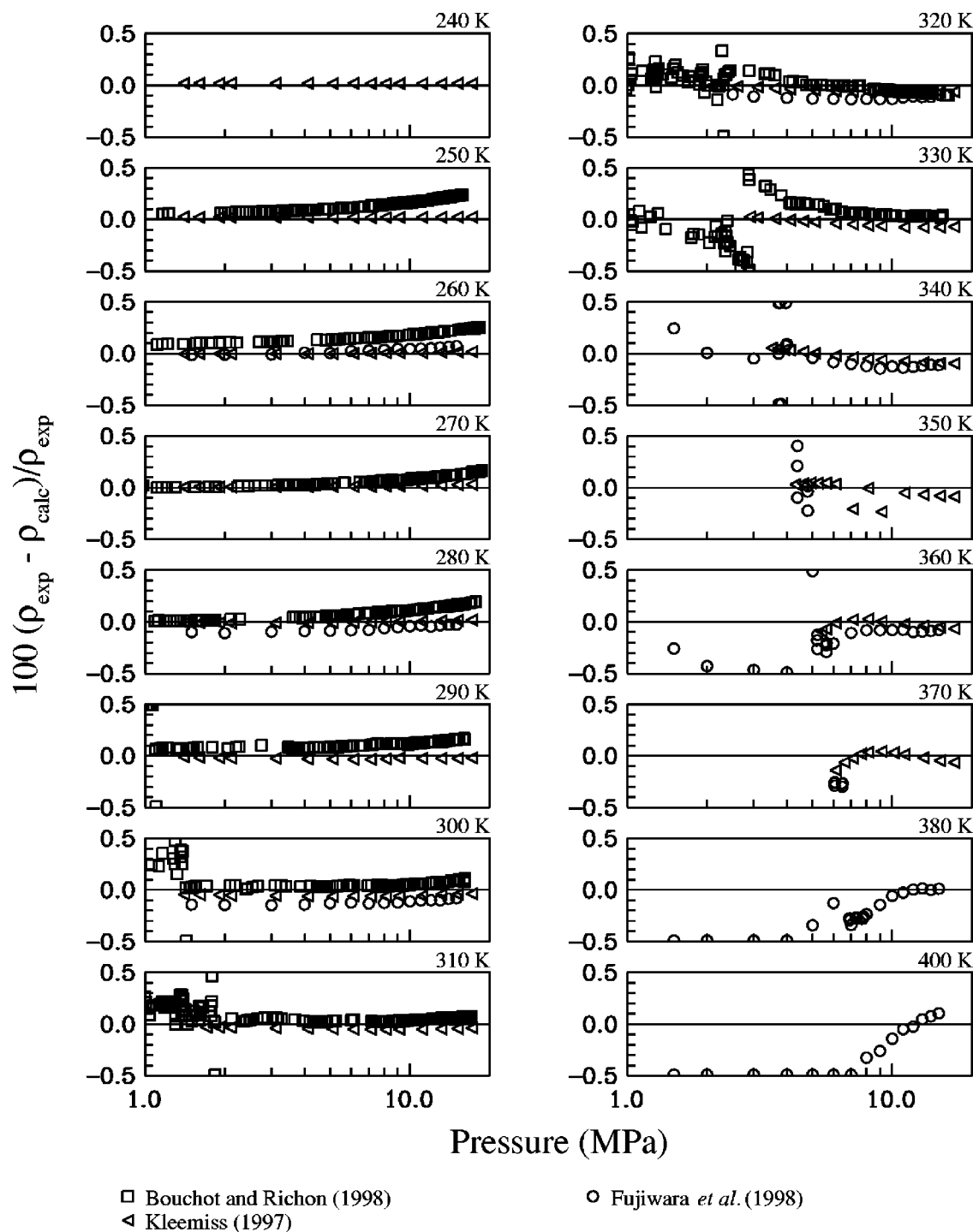


FIG. 12. Comparisons of densities calculated with the mixture model to experimental data for the R-125/134a/143a ternary mixture.

positive values) typical of previous equations of state within the two phase region. The two equations represent the liquid and vapor densities for the pure fluid with nearly the same deviations, but because recently measured data were not available to Sunaga *et al.*, comparisons in the critical region are better for the equation of Lemmon and Jacobsen. Comparisons of the experimental data for the R-32/125 binary mixture showed similar trends in density in the liquid and vapor phases at temperatures away from the critical point when the equation of Lemmon and Jacobsen was replaced by the equation of Sunaga *et al.* However, at temperatures be-

tween 310 and 400 K differences ranged from 0.1% in density at pressures greater than 5 MPa to 0.5% in density at pressures between 2 and 5 MPa. At the critical point of R-410A (344.51 K, 4.9026 MPa), the calculated critical density differed by 17%. The equation of state of Lemmon and Jacobsen (2004) for R-125 should be used with the mixture equations presented here to obtain the uncertainties stated earlier for the mixture model.

Although calculated densities and heat capacities in the liquid and vapor are generally quite similar between the new mixture model presented here and the JSRAE model of

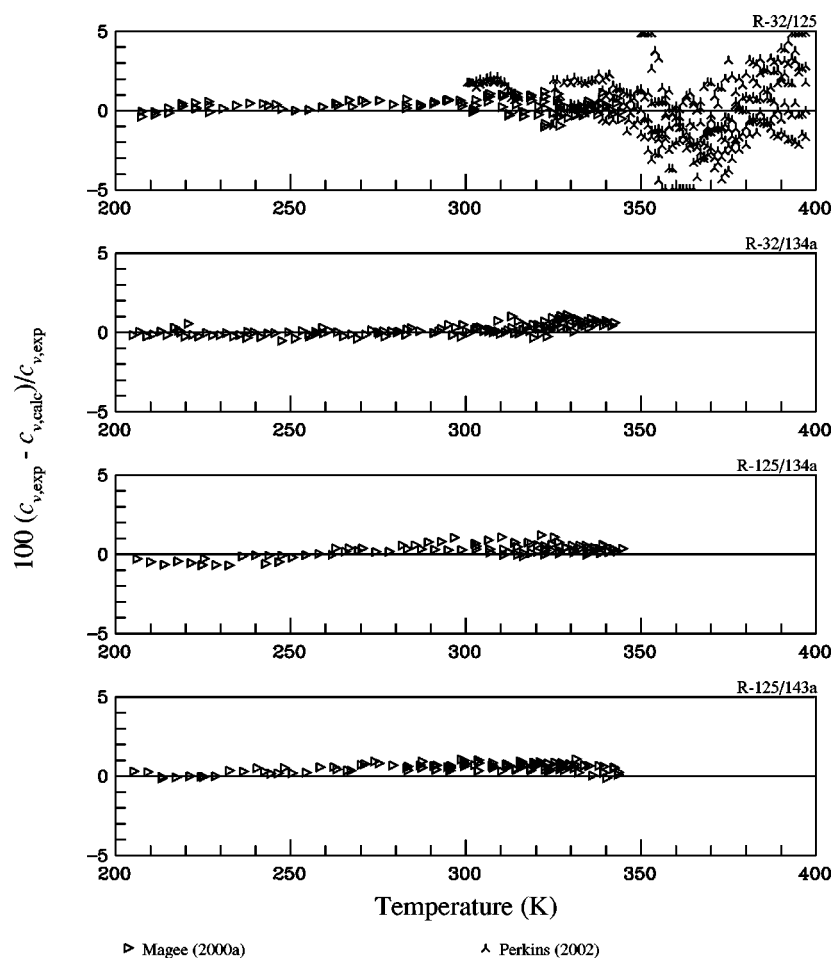


FIG. 13. Comparisons of isochoric heat capacities calculated with the mixture model to experimental data for the R-32/125, R-32/134a, R-125/134a, and R-125/143a binary mixtures.

Tillner-Roth *et al.* (1998), deviations in the critical region have been substantially improved by incorporating new experimental data that were not available to Tillner-Roth *et al.* For example, deviations for the older model exceed 0.5% in density at 330 K for the 0.7 R-32/0.3 R-125 mixture (for the data of Magee, 2002) as shown in Fig. 19, although the deviations are quite similar at a composition of 0.5/0.5 [for the data of Kleemiss (1997) and of Magee and Haynes (2000)]. For the data of Zhang *et al.* (1996), the equimolar data show similar comparisons, but higher deviations are observed at pressures near 3 MPa for the mixture containing 0.7 R-32/0.3

R-125. In addition, plots of excess volumes reveal several differences between these two models. In particular, for the R-32/125 mixture at 250 K and 5 MPa, Figs. 20 and 21 show excess volumes and excess enthalpies over the full composition range. Although the excess volumes are of similar magnitudes at compositions of R-32 above 0.5 mole fraction, the data of Benmansour and Richon (1999a) confirm that the excess volumes should be negative at mole fractions of 0.21 and 0.25 of R-32, as demonstrated by the new mixture model. The model of Tillner-Roth *et al.* shows systematic deviations for both the excess volume and excess enthalpy.

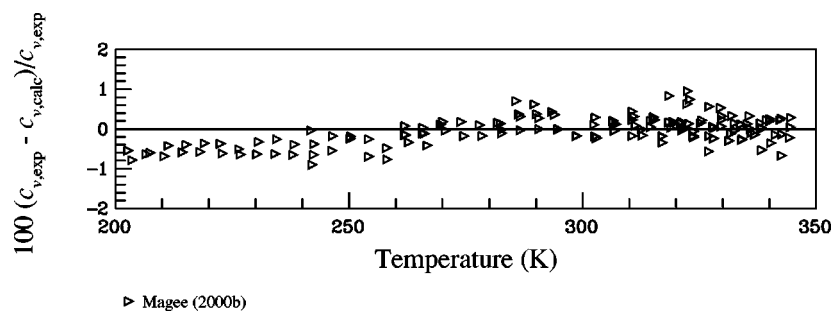


FIG. 14. Comparisons of isochoric heat capacities calculated with the mixture model to experimental data for the R-32/125/134a ternary mixture.

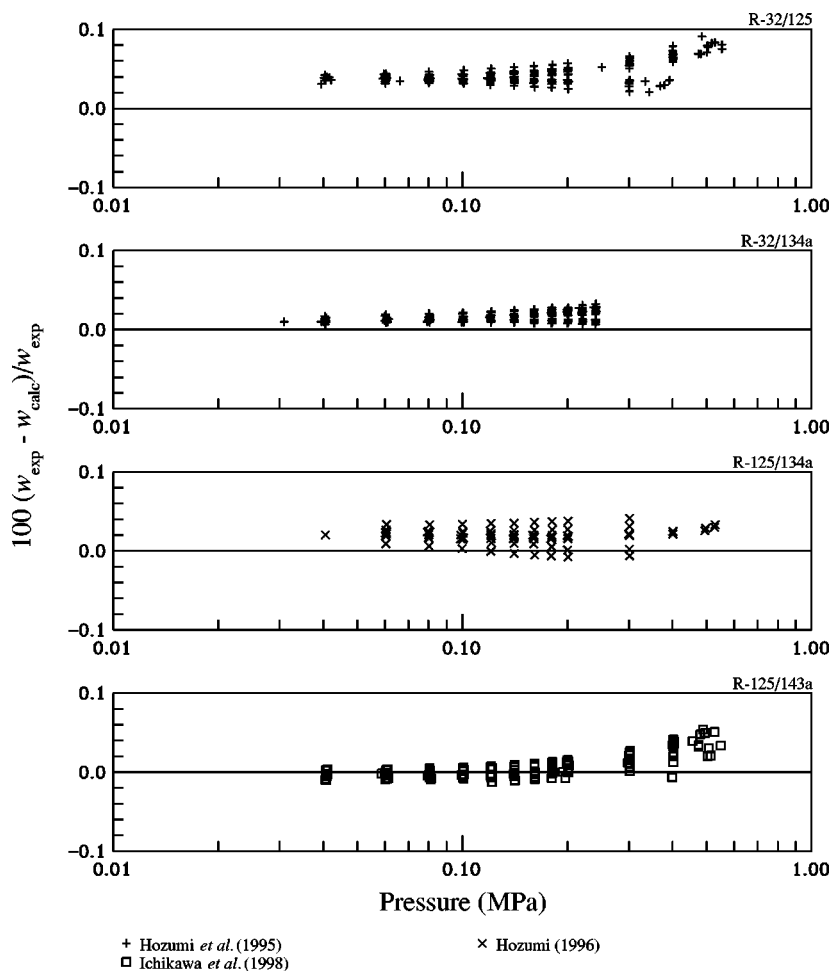


FIG. 15. Comparisons of the speed of sound in the vapor phase calculated with the mixture model to experimental data for the R-32/125, R-32/134a, R-125/134a, and R-125/143a binary mixtures.

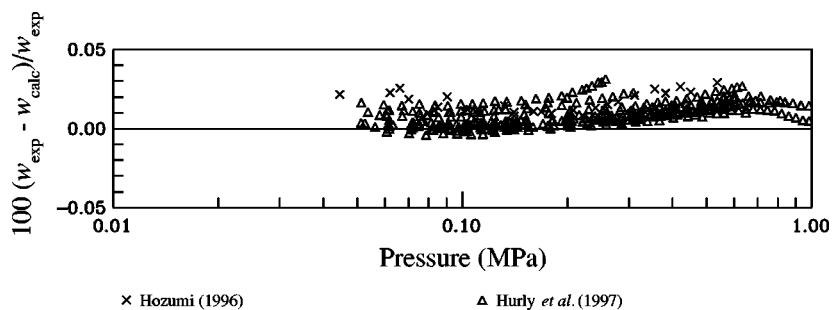


FIG. 16. Comparisons of the speed of sound in the vapor phase calculated with the mixture model to experimental data for the R-32/125/134a ternary mixture.

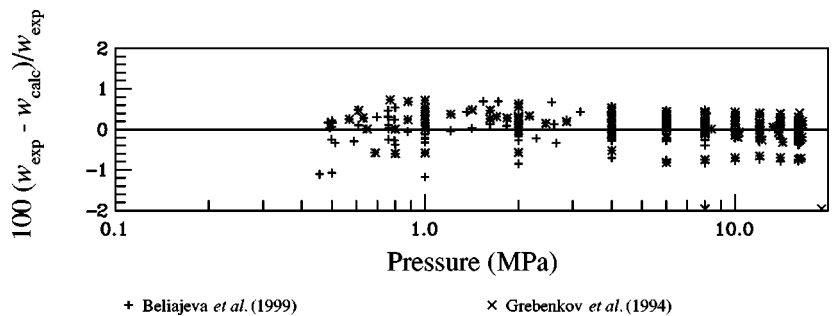


FIG. 17. Comparisons of the speed of sound in the liquid phase calculated with the mixture model to experimental data for the R-134a/152a binary mixture.

TABLE 6. Calculated property values for computer code verification

Mixture <sup>a</sup>	Temp. (K)	Density (mol/dm <sup>3</sup> )	Pressure (MPa)	Isochoric heat capacity (J/(mol-K))	Isobaric heat capacity (J/(mol-K))	Speed of sound (m/s)	Fugacity of first component (MPa)
50/50 R-32/125	300	13.	3.602 891	76.647 14	133.4161	410.3700	0.760 4262
	300	0.9	1.639 941	75.115 26	113.2553	145.0593	0.664 9367
	343	5.8	4.570 375	109.5538	8875.064	99.953 04	1.609 648
50/50 R-32/134a	300	15.	11.681 28	71.035 76	113.8506	615.0602	0.872 4334
	300	0.5	1.018 672	66.892 97	90.353 74	167.3402	0.450 8831
	364	5.9	4.958 696	101.7819	2496.022	112.4511	1.955 381
50/50 R-125/134a	300	11.	3.475 706	96.946 10	151.7337	438.1132	0.631 9712
	300	0.4	0.834 4532	88.878 44	108.8584	136.5385	0.367 5279
	358	4.9	3.992 433	127.6533	3295.904	86.673 45	1.467 750
50/50 R-125/143a	300	11.	7.371 538	91.511 91	141.3994	445.2289	0.708 4060
	300	0.7	1.303 202	88.849 67	121.2343	130.5114	0.526 7233
	344	4.9	3.756 290	122.3978	7882.864	86.752 97	1.251 023
50/50 R-134a/143a	300	12.	9.548 637	88.066 94	132.5006	546.5012	0.409 5593
	300	0.4	0.826 9971	81.911 78	102.7968	149.4877	0.346 9823
	362	5.1	4.051 228	118.3833	3725.227	94.848 13	1.175 577
50/50 R-134a/152a	300	13.	9.867 019	85.804 24	127.7686	644.0166	0.403 9289
	300	0.3	0.636 7737	76.512 68	95.584 40	161.7513	0.277 9604
	381	5.2	4.320 773	113.1712	7407.069	104.4937	1.414 853
33/33/34 R-32/125/134a	300	13.	7.889 929	81.346 85	129.4822	508.7768	0.547 0054
	300	0.5	1.023 377	75.543 10	97.923 34	151.3492	0.299 1716
	300	11.	2.309 797	92.743 34	148.5144	418.3732	0.389 4721
33/33/34 R-125/134a/143a	300	0.5	0.997 6918	86.918 85	111.2741	138.1841	0.281 5930

<sup>a</sup>Compositions are given in mole percent.

<sup>b</sup>Calculated state point is near the critical point.

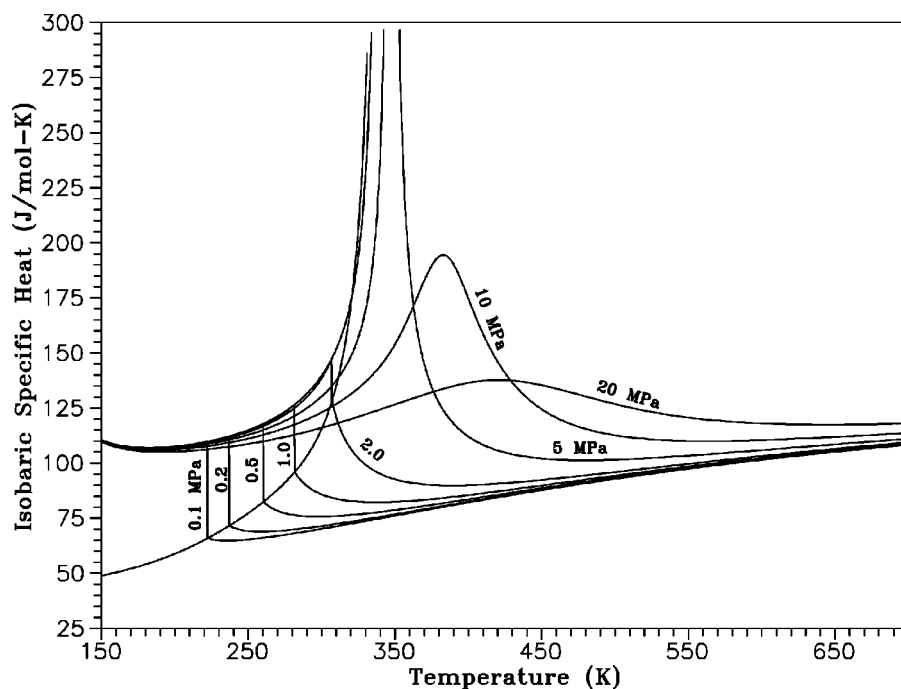


FIG. 18. Isobaric heat capacity versus temperature diagram for an equimolar mixture of R-32 and R-125.

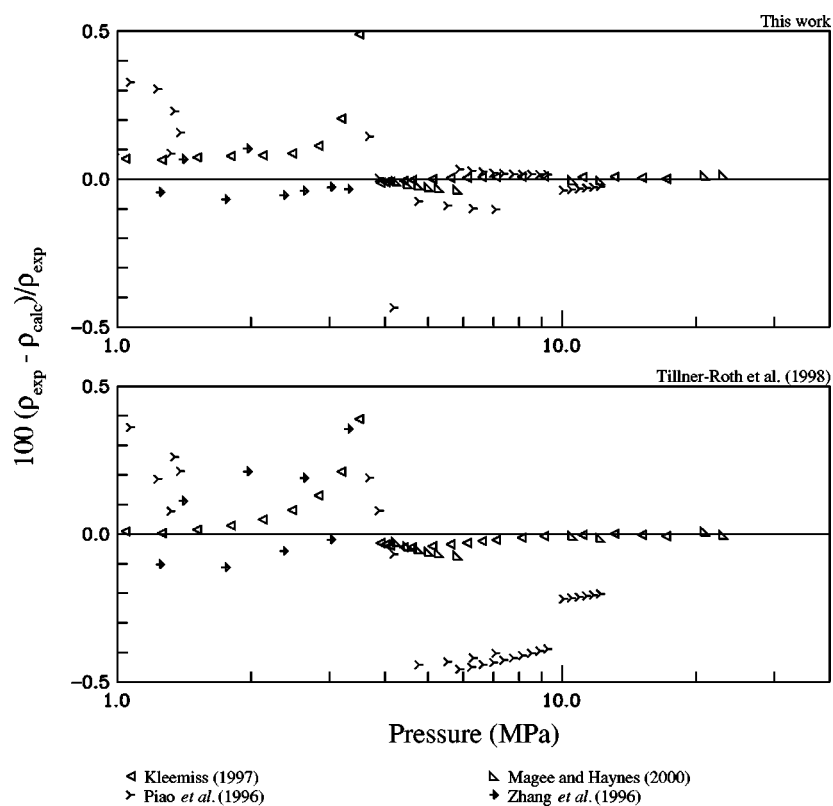


FIG. 19. Comparisons of densities calculated with the mixture model developed in this work and the mixture model of Tillner-Roth *et al.* (1998) to experimental data for the R-32/125 binary mixture at 330 K.

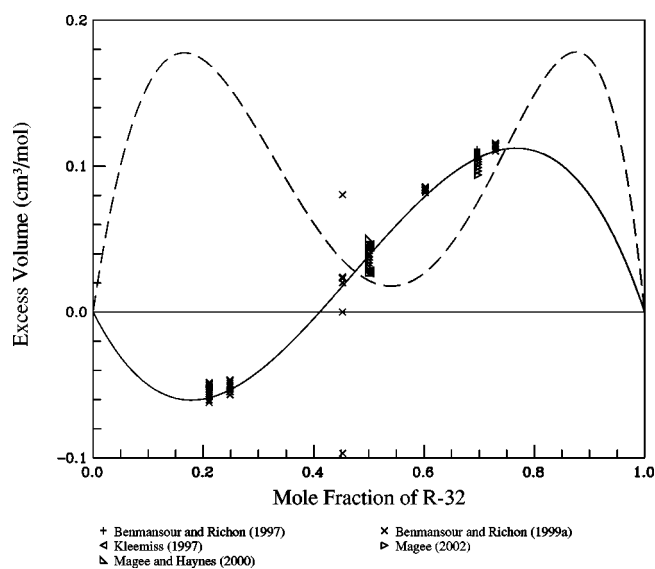


FIG. 20. Excess volumes for the R-32/125 binary mixture at 250 K and 5 MPa: (solid line) this work, (dashed line) mixture model of Tillner-Roth *et al.* (1998). Experimental data between 243 and 256 K are shown for comparison.

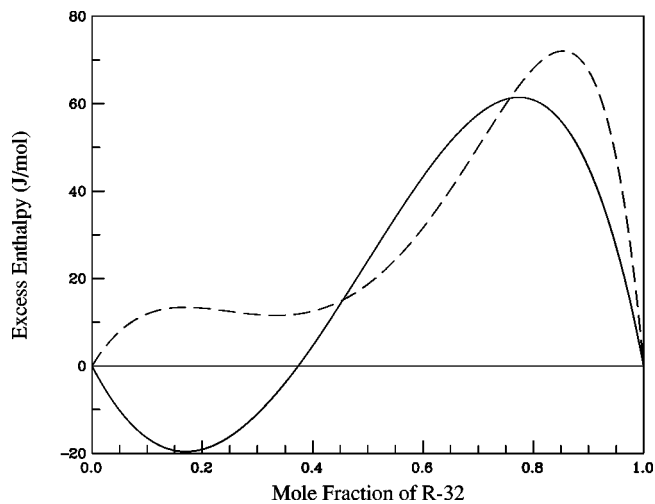


FIG. 21. Excess enthalpies for the R-32/125 binary mixture at 250 K and 5 MPa: (solid line) this work, (dashed line) mixture model of Tillner-Roth *et al.* (1998).

## 5. Acknowledgments

This work was funded by the 21-CR research program of the Air-Conditioning and Refrigeration Technology Institute; the Office of Building Technology, State and Community Programs of the U.S. Department of Energy. We thank Dr. Mark McLinden of NIST, Boulder, for his assistance and suggestions during the development and documentation of the equation.

## 6. References

- Beliajeva, O. V., A. J. Grebenkov, T. A. Zajatz, and B. D. Timofeev, *Int. J. Thermophys.* **20**, 1689 (1999).
- Benmansour, S. and D. Richon, *Int. Electron. J. Phys.-Chem. Data* **3**, 149 (1997).
- Benmansour, S. and D. Richon, *Int. Electron. J. Phys.-Chem. Data* **4**, 29 (1998).
- Benmansour, S. and D. Richon, *Int. Electron. J. Phys.-Chem. Data* **5**, 9 (1999a).
- Benmansour, S. and D. Richon, *Int. Electron. J. Phys.-Chem. Data* **5**, 55 (1999b).
- Benmansour, S. and D. Richon, *Int. Electron. J. Phys.-Chem. Data* **5**, 127 (1999c).
- Benmansour, S. and D. Richon, *Int. Electron. J. Phys.-Chem. Data* **5**, 117 (1999d).
- Bouchot, C. and D. Richon, *Int. Electron. J. Phys.-Chem. Data* **4**, 163 (1998).
- Chung, E. Y. and M. S. Kim, *J. Chem. Eng. Data* **42**, 1126 (1997).
- Defibaugh, D. R. and G. Morrison, *Int. J. Refrig.* **18**, 518 (1995).
- Dressner, M. and K. Bier, *Fortschr.-Ber. VDI* **3** (1993).
- Fujiwara, K., H. Momota, and M. Noguchi, 13th Japan Symp. Thermophys. Prop. **A11.6**, 61 (1992).
- Fujiwara, K., S. Nakamura, and M. Noguchi, *J. Chem. Eng. Data* **43**, 967 (1998).
- Grebenkov, A. J., Yu. G. Kotelevsky, V. V. Saplitza, O. V. Beljaeva, T. A. Zajatz, and B. D. Timofeev, *Proc. CFC's: The Day After, IIR Comm B1, B2, E1, E2*, p. 21 (1994).
- Gunther, D. and F. Steimle, *Int. J. Refrig.* **20**, 235 (1996).
- Higashi, Y., *Int. J. Thermophys.* **16**, 1175 (1995).
- Higashi, Y., *J. Chem. Eng. Data* **42**, 1269 (1997).
- Higashi, Y., *Int. J. Thermophys.* **20**, 1483 (1999a).
- Higashi, Y., *J. Chem. Eng. Data* **44**, 328 (1999b).
- Higashi, Y., *J. Chem. Eng. Data* **44**, 333 (1999c).
- Higuchi, M. and Y. Higashi, *Proc. 16th Japan Symp. Thermophys. Prop.*, Hiroshima, 1995, p. 5.
- Higuchi, M., private communication with Yukihiro Higashi, Dept. of Mech. Eng., Iwaki Meisei University, Japan, 1997.
- Holcomb, C. D., J. W. Magee, J. Scott, S. L. Outcalt, and W. M. Haynes, *Selected Thermodynamic Properties for Mixtures of R-32 (difluoromethane), R-125 (pentafluoroethane), R-134A (1,1,1,2-tetrafluoroethane), R-143A (1,1,1-trifluoroethane), R-41 (fluoromethane), R-290 (propane), and R-744 (carbon dioxide)*, National Institute of Standards and Technology, Tech Note 1397 (1998).
- Hozumi, T., private communication, Dept. of Mech. Eng., Keio University, Yokohama, Japan, 1996.
- Hozumi, T., H. Sato, and K. Watanabe, 4th Asian Thermophysical Properties Conference, Japan, 1995, p. 307.
- Hurly, J. J., J. W. Schmidt, and K. A. Gillis, *Int. J. Thermophys.* **18**, 655 (1997).
- Ichikawa, T., K. Ogawa, H. Sato, and K. Watanabe, *Speed-of-Sound Measurements for Gaseous Pentafluoroethane and Binary Mixture of Pentafluoroethane + 1,1,1-Trifluoroethane*, Department of System Design Engineering, Faculty of Science and Technology, Keio University, Yokohama, Japan, 1998.
- Ikeda, T. and Y. Higashi, *Proc. 16th Japan Symp. Thermophys. Prop.*, Hiroshima, 1995, pp. 169–172.
- Kato, R., K. Shirakawa, and H. Nishiumi, *Fluid Phase Equilib.* **194**, 995 (2002).
- Kim, C.-N., E.-H. Lee, Y.-M. Park, J. Yoo, K.-H. Kim, J.-S. Lim, and B.-G. Lee, *Int. J. Thermophys.* **21**, 871 (2000).
- Kim, C.-N. and Y.-M. Park, *Int. J. Thermophys.* **20**, 519 (1999).
- Kishizawa, G., H. Sato, and K. Watanabe, *Int. J. Thermophys.* **20**, 923 (1999).
- Kiyoura, H., J. Takebe, H. Uchida, H. Sato, and K. Watanabe, *J. Chem. Eng. Data* **41**, 1409 (1996).
- Kleemiss, M., *Fortschr.-Ber. VDI* **19** (1997).
- Kleiber, M., *Fluid Phase Equilib.* **92**, 149 (1994).
- Kubota, H. and T. Matsumoto, *J. Chem. Eng. Jpn.* **26**, 320 (1993).
- Laesecke, A. *Int. J. Refrig.* (submitted, 2004).
- Lemmon, E. W., A. Generalized Model for the Prediction of the Thermodynamic Properties of Mixtures Including Vapor-Liquid Equilibrium, Ph.D. dissertation, University of Idaho, Moscow, 1996.
- Lemmon, E. W. and R. T. Jacobsen, *Int. J. Thermophys.* **20**, 825 (1999).
- Lemmon, E. W. and R. T. Jacobsen, *J. Phys. Chem. Ref. Data* **29**, 521 (2000).
- Lemmon, E. W. and R. T. Jacobsen, *A New Functional Form and Fitting Techniques for Equations of State with Application to Pentafluoroethane (HFC-125)*, *J. Phys. Chem. Ref. Data*, (submitted, 2004).
- Lemmon, E. W., R. T. Jacobsen, S. G. Penoncello, and D. G. Friend, *J. Phys. Chem. Ref. Data* **29**, 331 (2000).
- Lemmon, E. W. and M. O. McLinden, *Method for Estimating Mixture Equation of State Parameters*, Proceedings of the Thermophysical Properties and Transfer Processes of New Refrigerants Conference, Paderborn, Germany, 2001, pp. 23–30.
- Lemmon, E. W., M. O. McLinden, and M. L. Huber, *NIST Standard Reference Database 23: Reference Fluid Thermodynamic and Transport Properties-REFPROP, Version 7.0*, National Institute of Standards and Technology, Standard Reference Data Program, Gaithersburg (2002).
- Lemmon, E. W. and R. Tillner-Roth, *Fluid Phase Equilib.* **165**, 1 (1999).
- Li, J., R. Tillner-Roth, H. Sato, and K. Watanabe, *Int. J. Thermophys.* **20**, 1639 (1999).
- Lim, J. S., J.-Y. Park, B.-G. Lee, and Y.-W. Lee, *Fluid Phase Equilib.* **193**, 29 (2002).
- Lisal, M. and V. Vacek, *Fluid Phase Equilib.* **118**, 61 (1996).
- Magee, J. W., *Int. J. Thermophys.* **21**, 95 (2000a).
- Magee, J. W., *Int. J. Thermophys.* **21**, 151 (2000b).
- Magee, J. W. (private communication, NIST, Boulder, Colorado, 2002).
- Magee, J. W. and W. W. Haynes, *Int. J. Thermophys.* **21**, 113 (2000).
- Nagel, M. and K. Bier, *Int. J. Refrig.* **18**, 534 (1995).
- Nagel, M. and K. Bier, *Int. J. Refrig.* **19**, 264 (1996).
- Oguchi, K., K. Amano, T. Namiki, and N. Umezawa, *Int. J. Thermophys.* **20**, 1667 (1999).
- Oguchi, K., T. Takaishi, N. Yada, T. Namiki, and T. Sato (private communication, Kanagawa Institute of Technology, Japan, 1995).
- Outcalt, S. L. and M. O. McLinden, *J. Phys. Chem. Ref. Data* **25**, 605 (1996).
- Perkins, R. A. (private communication, NIST, Boulder, Colorado, 2002).
- Piao, C.-C., I. Iwata, and M. Noguchi (private communication, Mech. Eng. Lab., Daikin Industries, Ltd., Japan, 1996).
- Sand, J. R., S. K. Fischer, and J. A. Jones, *Int. J. Refrig.* **17**, 123 (1994).
- Sato, T., H. Kiyoura, H. Sato, and K. Watanabe, *J. Chem. Eng. Data* **39**, 855 (1994).
- Sato, T., H. Kiyoura, H. Sato, and K. Watanabe, *Int. J. Thermophys.* **17**, 43 (1996).
- Schramm, B., J. Hauck, and L. Kern, *Ber. Bunsenges. Phys. Chem.* **96**, 745 (1992).
- Shimawaki, S., K. Fujii, and Y. Higashi, *Int. J. Thermophys.* **23**, 801 (2002).
- Sunaga, H., R. Tillner-Roth, H. Sato, and K. Watanabe, *Int. J. Thermophys.* **19**, 1623 (1998).
- Tack, A. and K. Bier, *Fortschr.-Ber. VDI* **3**, 1 (1997).
- Takagi, T., T. Sakura, T. Tsuji, and M. Hongo, *Fluid Phase Equilib.* **162**, 171 (1999).
- Tillner-Roth, R., *J. Chem. Thermodyn.* **25**, 1419 (1993).
- Tillner-Roth, R. and H. D. Baehr, *J. Phys. Chem. Ref. Data* **23**, 657 (1994).
- Tillner-Roth, R., J. Li, A. Yokozeki, H. Sato, and K. Watanabe, *Thermodynamic Properties of Pure and Blended Hydrofluorocarbon (HFC) Refrigerants* (Japan Society of Refrigerating and Air Conditioning Engineers, Tokyo, 1998).

- Tillner-Roth, R. and A. Yokozeki, *J. Phys. Chem. Ref. Data* **25**, 1273 (1997).
- Tuerk, M., M. Crone, and K. Bier, *J. Chem. Thermodyn.* **28**, 1179 (1996).
- Uchida, H., H. Sato, and K. Watanabe, *Int. J. Thermophys.* **20**, 97 (1999).
- Weber, F., *Fluid Phase Equilib.* **174**, 165 (2000).
- Weber, L. A. and D. R. Defibaugh, *Int. J. Thermophys.* **15**, 863 (1994).
- Widiatmo, J. V., T. Fujimine, H. Sato, and K. Watanabe, *J. Chem. Eng. Data* **42**, 270 (1997).
- Widiatmo, J. V., H. Sato, and K. Watanabe, *High Temp.-High Press.* **25**, 677 (1993).
- Widiatmo, J. V., H. Sato, and K. Watanabe, *Int. J. Thermophys.* **16**, 801 (1994a).
- Widiatmo, J. V., H. Sato, and K. Watanabe, *Fluid Phase Equilib.* **99**, 199 (1994b).
- Yokoyama, C., T. Nishino, and M. Takahashi, *Fluid Phase Equilib.* **174**, 231 (2000).
- Zhang, H.-L., H. Sato, and K. Watanabe, *J. Chem. Eng. Data* **41**, 1401 (1996).
- Zhang, H.-L., S. Tada, H. Sato, and K. Watanabe, *Fluid Phase Equilib.* **151**, 333 (1998).